ADDIS ABABA UNIVERSITY

SCHOOL OF GRADUATE STUDIES

INSTITUTE OF TECHNOLOGY

DEPARTMENT OF MECHANICAL ENGINEERING

Analysis of Wheel/Rail Contact Geometry and Applied Load Conditions on the Rail Head Surface

A Thesis Submitted to the Graduate School of Addis Ababa University in Partial Fulfillment of the Requirements for the Degree of Masters of Science

In

Mechanical Engineering

(Mechanical Design)

By

Addisu Negash

Advisor

Dr. Daniel Tilahun

October, 2012

ADDIS ABABA UNIVERSITY

SCHOOL OF GRADUATE STUDIES

INSTITUTE OF TECHNOLOGY

DEPARTMENT OF MECHANICAL ENGINEERING

Analysis of Wheel/Rail Contact Geometry and Applied Load Conditions on the Rail Head Surface

By

Addisu Negash

October, 2012

Approved by Board of Examining:

Daniel Tilahun (Dr.)	_____	_____
Chairman	Signature	Date
Daniel Tilahun (Dr.)	_____	_____
Advisor	Signature	Date
Zewudu Abdi (Dr.-Ing)	_____	_____
Internal Evaluator	Signature	Date
Tamirat Tesfaye (Dr.-Ing)	_____	_____
External Evaluator	Signature	Date

Acknowledgement

First of all I would like to thank my advisor Dr.Daniel Tilahun for his grateful support and continuous advice of the work from the beginning up to the final result of the paper. I want to appreciate also his willingness and giving of motivations to work on research areas focusing on the current situations of the country, Ethiopia, pointing its future development and related problems to lay down the possible respective solutions.

I would like to thank also to all people who stand on my side during the work of the paper. Especially to Abdulhakim Shukurea and Ephrem Zeleke, friends and colleagues who support and guide me during the complex mathematical modeling of wheel/rail contact geometry.

Thanks also to engineer Yonus who is the mechanical engineer at Ethiopian Railway Corporation and helped me by giving the necessary materials and advice to manage the possible outcomes of the research.

Finally, special thanks to my friend Abebech Abera for her patience, advice, support and motivation standing always on my side for the successful accomplishment of this paper and for the success of my life at all.

Abstract

Now a day the railway transport infrastructure in Ethiopia is the major issues in relation to the development of the country. To strengthen this infrastructure, related researches must be conducted at the beginning of the construction of the sector. This paper which mainly concerned about the analysis of wheel/rail contact is done to predict and minimize failures caused by improper wheel/rail contact.

The objective of this research is to determine the optimum wheel/rail contact and to identify the position of contact, which is basic to justify the way of load distribution on the contacting interface.

In this paper the analysis of wheel/rail contact is based on the X, Y, and Z coordinate systems. With the help of these coordinates the type and place of contact on the wheel/rail interface and the way of stress distribution on the rail head surface is identified. Throughout the whole wheel/rail contact analysis, the Hertz contact theory assumptions are basically considered. Therefore based on Hertz contact theory and analytical results (mathematical models developed), the type of contact between wheel and rail is identified as point contact. The positions of the contact point is on the center of rail head where the rail lateral surface parameter $S_2{}^r = 0$ and varies across the wheel lateral surface depending on the position and arrangement of the wheelset. During the analysis of wheel/rail contact the parameters considered are axle load, wheel and rail profiles. By using these parameters the maximum pressure applied throughout the contact point is calculated to be 794.9 MPa. From MATLAB (7.6) and ANSYS (13) simulation results the main failure causes due to maximum pressure applied are principal and shear stresses having their own direction of application on the rail head surface under axle load applied. The shape of the contact patch on the rail head surface is elliptical. The shape identified is practically matched with the assumptions taken from Hertz contact theory. However the size of elliptical patch depends on the size of load applied. The stress distribution throughout the area of contact patch and the neighboring surfaces depends also on the size and direction of applied load.

Keywords: wheel/rail contact, maximum pressure, and railhead stresses

Contents

List of Tables

List of Figures

Nomenclatures

$S_1{}^w$: Wheel lateral surface parameter
$S_2{}^w$: Wheel longitudinal surface parameter
$S_1{}^r$: Rail longitudinal surface parameters
$S_2{}^r$: Rail lateral surface parameters
S: The projected arc length
C_H: The horizontal curvature
S: The actual arc length
θ: The development angle
t_1: Longitudinal unit tangent vectors
t_2: Lateral unit tangent vectors
$\overrightarrow{\mathrm{u^r}}$: The position of arbitrary point on the rail surface relative to the fixed global coordinate system
$\overrightarrow{\mathrm{R^{rp}}}$: The position of the origin of the rail profile coordinate system
$\overrightarrow{\mathrm{A^r}}$: The rotational transformation matrix used to show the orientation of the rail profile coordinate
$\overrightarrow{\mathrm{u^{rp}}}$: The location of the point **P** relative to the rail profile coordinate system
r^w: The position of arbitrary point on the wheel surface relative to the fixed global coordinate system
R^w: The position of the origin of the wheel profile coordinate system
A^w: The rotational transformation matrix used to show the orientation of the wheel profile coordinate system
u^w: The location of the point **P** relative to the wheel profile coordinate system
$g(s_1{}^w)$: The function that defines the wheel profile
σ_3: Maximum principal stresses three
σ_2: Principal stresses two
σ_1: Principal stresses one
τ_{max} : Maximum shear stress
a: Major semi-axis (ellipse) of contact patch
b: Minor semi-axis of contact patch ellipse

K_w: Constants that depend on the material properties of wheel

K_r: Constants that depend on the material properties of rail

K_3: Geometrical properties of both wheel and rail

$R_1{}^w$: The principal rolling radius of the wheel

$R_1{}^r$: The principal rolling radius of the rail

$R_2{}^w$: The principal transverse radius of curvature of the wheel

$R_2{}^r$: The principal transverse radius of curvature of the rail

P: Contact pressure

m&n: Hertz coefficients

Z: Contact point depth

UIC: International union of railways

Chapter 1

1. Introduction

1.1. Background of the Research

According to ____., [18], the history of rail transport dates back nearly 500 years and includes systems with man or horse power and rail of wood or stone. In 1604, the first railway in Britain was built, but it was called a wagonway and it was made of wood. Modern rail transport systems first appeared in England in the 1820s. These systems, which made use of the steam locomotive, were the first practical forms of mechanized land transport, and they remained the primary form of mechanized land transport for the next 100 years. By 1900, the railway was mostly completed, and there were more than a hundred train companies in Great Britain. In 1904, an engine called 'The City of Truro' became the first to travel at more than 100 miles an hour. The electrification of the railways began in 1933. This means that the trains began to run on electricity instead of steam. Railways were originally intended to carry mostly goods rather than passengers but in the 1970s, the value of carrying passengers overtook goods for the first time.

According to _____., [19] the railway lines construction in Ethiopia was first started in October 1897 from Djibouti in the period of Emperor Menelek II. The first commercial service began in July 1901, from Djibouti to Dire Dawa. By 1915 the line reached Akaki, only 23 kilometers from the capital, and two years later came all the way to Addis Ababa itself. Transportation infrastructure in Ethiopia has been neglected for decades, but is now a priority of the government of Ethiopia.

The railway transport system is one of the most crucial transport systems in the world with very high speed, safety and durability. Now a day, there is a high demand of railway transportation systems in the world including in our country Ethiopia for a long distance transport of passengers and goods. To satisfy such demands, it needs to have a railway transportation system with standard safety, comfort to customers, and reliable to user's etc. Such demands need the advanced design and analysis of functional components, which have a direct or an indirect impact on the customers and users demand. Among those many complex analyses this paper analyzes the wheel/rail interactions particularly on the wheel/rail contact profile and applied load conditions on the rail head surface. This research mainly

concentrates on searching of the contact points on the rail head to show the applied load conditions due to the axle load acted by the wheel from the railway vehicle.

After having a built up of trains with a relevant rail track systems, there is a periodic maintenance schedule. Due to the applications of different load cycles, relative rolling sliding motion of wheels on rail tracks, inappropriate geometrical fitness of wheel/rail contact profile and some other factors the maintenance schedule mainly concerns about the wheel/rail interaction systems. To reduce such maintenance costs it is better to analyze and understand the wheel/rail contact profile behavior and applied load conditions. The analysis of wheel/rail contact profile requires the detail analysis of the contacting surface conditions and factors affecting the contacting surface behavior of the two machine components (rail-wheel). Therefore to understand the general functions and properties of the two machine components (wheel/rail), it is preferable to see each sub components separately as follows.

1.1.1. Railway Track

It is laid on the appropriate ground level and geographical sites based on the appropriate design specification. It has different components interrelated with meaningful arrangements for the general railway dynamic operations. Rail track is a fundamental part of railway infrastructure and its components can be classified into two main categories: superstructure and substructure. The most obvious parts of the track as the rails, rail pads, sleepers, and fastening systems are referred to as the superstructure while the substructure is associated with a geotechnical system consisting of ballast, sub-ballast and sub grade (formation). Both superstructure and substructure are mutually important in ensuring the safety and comfort of passengers and quality of the ride [1]. The typical shape and construction profiles of a ballasted track are illustrated in figure 1.1.

The rail track sleeper is used to transmit the wheel load to the ballast medium. In addition, it has functions such as maintaining track alignment and gauge, restraining longitudinal and lateral rail movements, and providing strength and stability to track structure [3]. The rail joints are used to join rails depending on the required position of the rails.

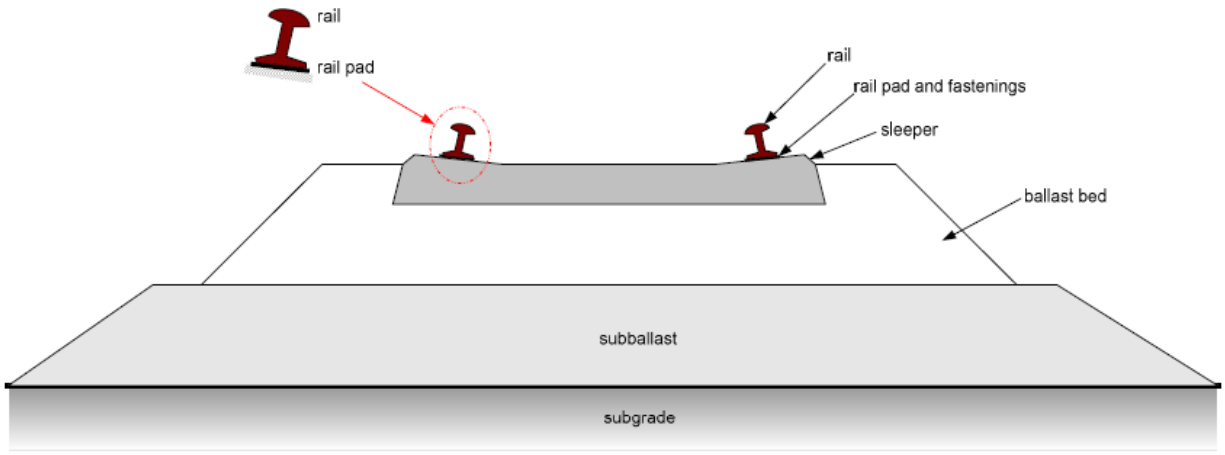

Figure 1.1: Rail track components and their arrangements

During the interaction between the wheel set and the rail track there are different conditions created on the contacting surface. These dynamic contact behaviors depend partly on the track geometry. The most common track geometries having great impact on the railway vehicle dynamic behavior are:

- Track gauge: the distance between the right and left rail inner gauge corners
- Track cant (supper elevation): the difference between the level of the two rail on a curve
- Track curvature: it is the inverse of the radius of the curved track
- Rail head: it is the surface of the rail having a direct contact to the railway vehicle wheel set.
- Wheel and rail tread profile

By managing those geometrical parameters of the track it is possible to control the dynamic behaviors of the wheel-rail dynamic contact, especially on the curved track.

1.1.2. Wheel set

The wheel set is placed attached to the railway bogie. Bogie is a structure underneath a train to which axles and hence wheels are attached through bearings. Bogies are classified according to their configurations in terms of the numbers of axles, the design and structure of the suspension systems. Bogies serve a number of purposes.

- ✓ Support of the rail vehicle body.
- ✓ Provides stability on both straight and curved track.

- ✓ Ensures ride comfort by absorbing vibration and minimizing centrifugal forces when the train runs on curves at high speed.
- ✓ Minimizes generation of track irregularities and rail abrasion

A wheel set comprises of two wheels rigidly connected by a common axle and it provides:

- The appropriate distance between the vehicle and the track
- The guide to the motion of vehicles on the tracks
- The means of transmitting axle loads, traction and braking forces to the rails to accelerate and decelerate the vehicle etc.

Generally the railway wheel set has 6 degrees of freedom broadly classified as translational and rotational degrees of freedom. The translational degrees of freedom comprise three components that is translation along:

- X-axis
- Y-axis
- Z-axis

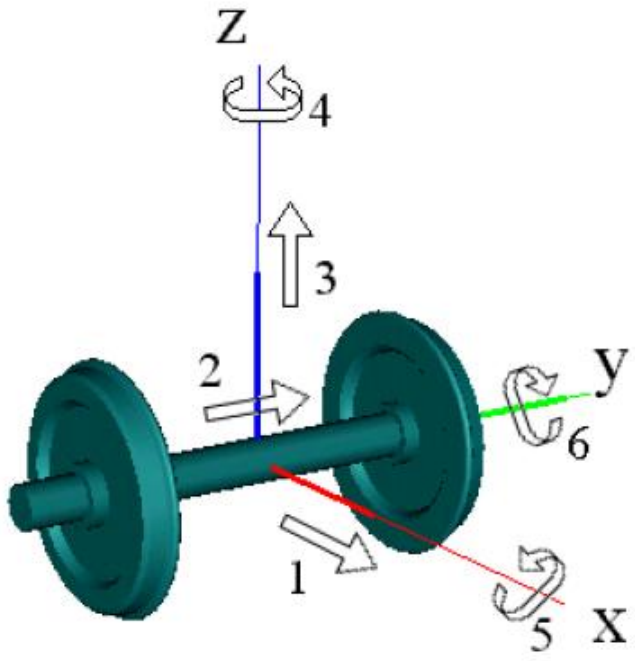

Figure1.2: Wheel set degrees of freedom

Similarly the rotational degrees of freedom consist of three components that is rotation about:

- X-axis
- Y-axis
- Z-axis

In conventional railway vehicles the wheels, assembled in a wheel set, are not free to rotate independently. Hence, their treads are coned in order to allow them to negotiate curves without slipping. However, it is recommended to reduce the wheel/rail conicity to allow wheel sets to remain stable up to much higher mileages, and to minimize contact between the flange root of the wheel and the gauge corner of the rail [5].

Performance, safety and maintenance cost strongly depend on the wheel set dynamics and particularly on how good is design of wheel and rail profiles. Using geometrical characteristics of a contact between wheel and rail it is possible to judge about dynamic parameters of wheel set and ultimately parameters of vehicle since a wheel set represents a source of disturbances from track to vehicle. The wheel-rail geometry plays a dominant role in vehicle lateral dynamics. The rolling radii, contact angles and the wheel set roll angle vary as the wheel set moves laterally relative to the rails. The nature of the functional dependency between these geometrically constrained variables and the wheel set lateral position depends on the wheel and rail cross-sectional shape [4].

The formulation of the wheel-rail contact problem is a complex task since it requires the study of the contact geometry, which is the problem of determining the location of the contact point on the profiled surfaces of the bodies, of the contact kinematics, which involves the calculation of normalized relative velocities at the point of contact, and of the contact mechanics, which is the problem of determining the contact forces [6].

The spatial distribution of contact forces caused by the form of tread surfaces of a wheel and a rail is the reason of a differential creep in contacts and occurrence of moving resistance forces. Schematically, the point-to-point contact is a statically indefinable system with a parameter of non definability, equal to a unit. Therefore, in mathematical modeling of distribution of loadings in contacts it is necessary to take deformations of contact areas into account.

The geometrical parameters of the point-to-point contact in the numerical integration of the equations of wheel set movement are defined as a result of coordinate analysis of contact points of wheels with rails. The radiuses of tread contact surfaces and profiles grade in points of contacts are related to such parameters [1].

1.1.3. Rail

Railway lines are made of straight sections and curves. Train driving on the curves essentially differs from that one on straight sections. On the curves railway gauge is widened (when curve radius is less than 350 m), and cant are mounted [11].

Rails are longitudinal steel members that are placed on spaced sleepers to guide the rolling stock [7]. Support of traffic load and guidance of vehicles are the two main tasks of the rails. For both tasks the correct contact geometry between wheel and rail is essential [16]. In addition to that rails are used to accommodate and transfer the wheel/axle loads into the supporting sleepers. The most commonly used profile is flat-bottom rail and is divided into three parts:

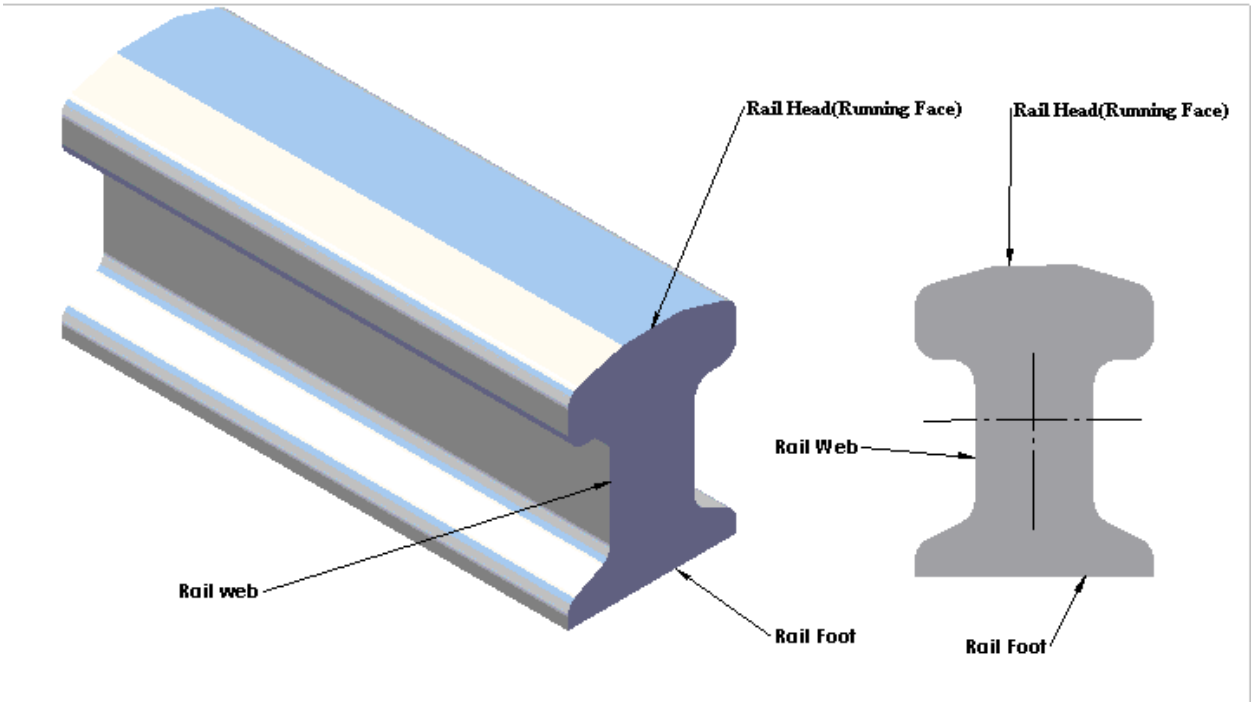

Figure 1.3: Flat bottom rail parts

- Rail head: the top surface that contacts with the wheel
- Rail web: the middle part that supports the rail head, like columns
- Rail foot: the bottom part that distributes the load from the web to the underlying superstructure components.

1.1.4. Rail-Wheel Interaction

The dynamic behavior of railway vehicle is greatly affected by the rail-wheel dynamic interactions. This interaction (wheel/rail) mainly depends on wheel/rail contact geometry. The changes in contacting geometry of rail/wheel depends on different parameters like the variation of wheel and rail profile, track gauge, rail inclinations, railhead surface irregularities, and flexibility of rail support. The main parameters influencing the wheel rail contact geometry are the profiles of wheels and rails, rail inclination and track gauge [14]. In this paper some of the parameters listed above affecting the contact geometry are assumed to be constant. Analysis of the wheel/rail contact geometry by considering all affecting parameters will make it complex. Therefore for better understanding and analysis of the condition under consideration, the grouping of interrelated parameters will result meaningful final outputs. Considering the other parameters constant and giving attentions to the analysis of wheel rail contact profiles is the main work of this paper. The wheel/rail contact profile is characterized by using the equivalent conicity, contact angle, lateral movement of wheel set, the wheel/rail material properties (elasticity), axle load, vehicle speed and yaw angle.

In railway transport system, the difficult problem frequently occurred is in the interaction between wheel and rail. In particular, the complexity of the interface geometry and the general operating geometric parameters (wheel lateral movement, cant angle, wheel conicity, and wheel rail profile variation and irregularities) makes this interaction very complex. There are different approaches to analyze this complex interaction. Some researchers focus on the dynamic behavior and dynamic response of each component during complex operational interaction. However, finding the locations of point of contacts, and analyzing the manner of interaction are the very priority. Therefore the contact parameters (wheel/rail profile, rail inclinations, wheel conicity, wheel lateral movement and track gauge) are the main inputs for the analysis of interaction.

Any load from the train is assumed to be transmitted to the track through wheel and the rail head to the ballast without affecting the environment. However, the large portions of these forces are distributed /dissipated in the wheel railhead contact surfaces. Therefore, from this general idea it is possible to conclude that the main failure of railway transport system is on these interacting interfaces.

From the data observed in the developed countries using the railway transport system at a large extent, these failures are extremely a problem od developed world. This failure causes huge cost as a railway

wheel rail maintenance and renewal. As stated above this is due to high stresses at the wheel rail interfaces, which causes failure like wear, fatigue and a combination of the two.

Understanding of interaction between these surfaces indicates and predicts the way how to treat them and how to prevent them from failures which is a better guide to select the appropriate materials, geometry, design, orientation etc. That is why this paper mainly concerns about the analysis of wheel rail contact profile and applied load condition on the rail head surface. The figure below shows the general wheel rail interactions from the front and side view respectively.

A) B)

Figure 1.4: Front views (A), and side view (B) of wheel/rail contact interface

Generally the main objective of this research is to find optimum solution to the wheel rail interaction which increases the safety and durability of these components. It is by indicating and showing the point of contact, contact patches and load distribution which is guidance for the future analysis of the system. The wheel rail interaction is mainly occurred between the wheel and the rail head surfaces. Both surfaces have a complicated geometry and micro structural complicated profiles. In addition to this the horizontal alignments of the track also affects the rail wheel dynamic interactions. These and other factors have increased the significance of this research.

1.2. Railway Transport Advantages and Disadvantages

1.2.1. Advantages

- ✓ Less energy utilization
- ✓ Less emission of CO_2
- ✓ Less use of land in transport
- ✓ Move massive amounts of "stuff" at one time.
- ✓ The cheapest mode of transporting major amounts of "stuff".
- ✓ Strengthen infrastructures thus lending to industrial based economies.
- ✓ Long distance travel and transport of bulky goods
- ✓ Encourages mobility of labor ad thereby provides a great scope for employment.

1.2.2. Disadvantages

- ✓ High noise emission
- ✓ Very rigid structure
- ✓ Difficult in communication
- ✓ Limited by geography.
- ✓ Requires a large investment of capital

1.3. Statement of the Problem

In wheel/rail contact analysis the main problem is identifying the type and position of contacts. However, the type and position of contacts depend on the standard materials and geometry of wheels and rails under consideration. Therefore, identification of wheel/rail standards and determination of their contacting geometry will be the first priority to identify and locate the type and position contacts respectively. Depending on the type and position of contacts, the way of distribution of cyclic axle load and its effects differs accordingly. Due to this, there are different questions to be answered, like:

- ✓ What types of loads (stresses) are induced on the contacting interface?
- ✓ How it is applied on the contacting interface?
- ✓ What are its consequences (effects)?

Such and other kinds of questions divert the interest of most researchers to direct their attentions to the area of contact mechanics, especially to wheel/rail contact problems.

1.4. Significance of the Research

This research has a great impact on future analysis and applications of wheel/rail contact in general and in particular in the Ethiopian context. Especially, it will contributes a lot for future analysis of wheel/rail contact failures like wear, fracture and instability showing the position of contact points and the way of load distributions on the contacting interface. Most practical wheel/rail contact installations are seen to be wearied out before the specified design periods. This may be due to improper installations and engagements of wheel/rail contacting surfaces. In addition to that it may be due to improper selection of wheel/rail materials and standard geometries. However, this paper provides the general wheel/rail contacting models and the appropriate contact types to optimize the problem on the contacting interface. In this paper the Hertz contact theory is considered for the analysis of wheel/rail contact. The Hertz contact theory is basically applicable for elastic materials and spherical, sphere to flat, and cylindrical contacts. The wheel/rail contact general profile is mostly a spherical or a sphere to flat contact depending on the standard profiles used. The material properties of wheel and rail are also considered as elastic, which is used to avoid brittle fracture and wears like abrasion on the rail head and wheel running surfaces. Due to that the Hertz contact theory is basically considered in this research throughout the paper.

1.5. Objective of the Research

1.5.1. Major Objective

The major objective of this research is determination of location of rail-wheel contact points and shape of contact patches on the rail profile with appropriate loading conditions.

1.5.2. Specific Objectives

- Determination of optimum rail wheel contact profile
- Determination of types of applied load and conditions
- Analysis of applied load (stress) distribution on the contacting surfaces

1.6. General Methodologies

To attain the optimum solution of wheel rail contact profile there are a step by step procedures that should be followed:

- Mathematical modeling of
  - ✓ Rail surface geometry
  - ✓ Wheel surface geometry
- Mathematical modeling of
  - ✓ Contact points
  - ✓ The shape of contact patches
  - ✓ Load distribution
- Simulation of a specific wheel rail contact

All the above formulations are conducted at a specified conditions and stated constraints with appropriate methodologies.

1.7. General Conditions

During the formulations of this paper the general conditions considered are based on the Hertz contact theory. These are:

- ✓ The surface of contacting bodies are assumed to be smooth
- ✓ the contact is assumed to be elastic
- ✓ isotropic and homogeneous material
- ✓ both contacting bodies were considered as half-spaces

1.8. General Parameters

During the analysis of wheel/rail contact there are different types of external and internal parameters affecting the interactions. These parameters can be broadly classified as:

- Vehicle parameters: vehicle type, operating speed, axle load, rail &wheel profile, conicity etc.
- Track parameters: Track geometry (gauge, cant, alignment and curve), Rail head profile and shape etc.
- Environmental parameters: Wheel /rail coefficient of friction conditions (dry, wet, contaminant etc.), wind force, soil property, forest around the railway track etc

In this paper all the above parameters are not taken into consideration due to its broad applications. Therefore most of the listed parameters are assumed to be constant except the rail head profile, wheel

profile, and axle load since the main aim of the research is to find and understand the effects of axle load and wheel rail geometrical relations on the wheel rail contacting surfaces.

Therefore in this paper common assumptions are made, that is:

- The rail wheel contact is assumed to be elastic contact that is there is no plastic deformation and time dependent variation of stress and strain during contact
- The material of rail and wheel is assumed to be identical (steel)
- No friction between contacts (Hertz contact theory)
- The analysis of the rail wheel contact at the macro level (no surface irregularities)
- No derailment occurred (nonlinearities due to rail-flange contact is assumed to be zero)

By considering such assumptions it is possible to avoid some complexity which is difficult to conduct without the use of some powerful computers and software packages. In this paper most of the analyses are based on analytical operations and simple input software simulations. Therefore at the beginning, avoiding some factors which induces the nonlinearities of dynamic interaction is the priority accordingly.

Chapter 2

2. Literature Reviews

2.1. Introduction

This is one of the portions of the paper that reviews the previous related works which are basic guide for the introduction of the current work. Some of them may have a direct relation with this work whereas the others may have indirect relations. But the main principles they have used and the major methodologies and approaches they precede will be selected generally and applied for the formulation of specific model and analysis.

Generally there are many journals, conference papers, proceedings, design works and books related to the railway engineering, railway vehicle dynamics and particularly wheel rail dynamics, contacts, interactions etc. but to save time and to manage the paper work the review of literatures mainly considers more related works to the paper. This intensifies the deep analysis of the previous related works and selection of appropriate conditions, approaches and methodologies for the successful accomplishment of the paper.

2.2. Wheel-Rail Contact

The history of wheel/rail contact mechanics is an integrated part of contact mechanics which goes back to the middle of the 19^{th} century. Problems of wheel/rail contact (damage phenomena and influence of contact mechanics on vehicle dynamics, especially on vehicle stability) have been investigated since the middle of the 19th Century. Knothe [10] studied that in 1855, Redtenbacher was the first to consider head checking. However, the scientific foundations of our present investigations are based on the work of Heinrich Hertz, Frederick William Carter and Hans Fromm. Basically the work of this paper is based on the Heinrich Hertz contact theory assumptions.

The Hertz contact theory leads to an elliptical contact area and a semi-ellipsoid contact pressure distribution in the contact region. Due to its efficiency and simplicity, this theory has been extensively applied since its publication. However, there are two limiting conditions for the applications of the Hertz contact theory [17]:

a) The contact between elastic bodies should be frictionless,

b) The significant dimensions of the contact area should be much smaller than the dimensions and the radii of curvature of the bodies in contact.

Contact is necessary in any engineering application to transfer force and power and hence it is an indispensable field of study. The major characteristics of contact mechanics are the localized deformation and the variation in the contact area with the contact force [17**]**. Being part of contact mechanics, the wheel/rail interactions encounters both localized deformation and contact area variation corresponding to the variation of the size of applied load.

Escalona [2] studied that the calculation of wheel-rail contact forces in the dynamic simulation of railroad vehicles involves the following steps:

1. Location of the position of the contact points on the surfaces of the wheel and rail.
2. Calculation of the normal contact forces.
3. Calculation of the tangential (creep) forces and moments

From the above three steps the first two steps are greatly essential for this research. Because in this paper the first priority is given to the analysis of the location of the contact point position on the rail head surface which is critical for the accuracy of the final output of the wheel/rail contact numerical results. In addition to that this paper gives high priority to the analysis and modeling of wheel/rail geometry which is basic to indicate the position of the contact point. Escalona [2] studied that the search of the contact points requires the surfaces of the wheel and rail to be mathematically parameterized.

Different researchers use different approaches to analyze the wheel/rail contact surface geometry and to indicate the position of contact points. Matsumura [15] use table-update and table-interpolation algorithms on the accurate analysis of vehicle/turnout interactions. Based on this method for modeling change in the rail cross-section, multiple look-up contact tables can be used. The numerical procedure of using multiple look-up contact tables can be classified into two different approaches. In the first approach, changes in the rail cross-section around the neighborhood of the contact point are assumed to be small, and the contact table used to determine the location of contact points is discontinuously changed as a function of the distance the wheel set traveled. Since only small modifications are required, the simulation of vehicle/turnout interactions can be performed in a straightforward manner. However, since discontinuations change in contact points are inevitable due to the discontinuous table updating, a large number of look-up contact tables need to be prepared in advance for reliable simulations.

In the second approach, on the other hand, the location of contact point is determined by interpolating nearest two look-up contact tables. That is, the location of contact point that should be obtained using interpolated rail profiles can be determined using interpolation of two contact tables.

Karwacki [8] studied that in the elastic approach, no kinematic contact constraints are imposed; the wheel has six degrees of freedom with respect to the rail; and small penetrations at the contact points are allowed. In the elastic contact formulations, a compliant force element that consists of stiffness and damping forces is used to determine the normal contact force.
In this method, the location of the contact points is determined by solving a set of algebraic equations. For each contact, four algebraic equations are solved to determine the four parameters that describe the geometry of the wheel and the rail surfaces.

2.3. Wheel/Rail Contact Stress

The stress field created by the contact stresses was first introduced by Heinrick Hertz in 1881. Assessment of contact stresses at the wheel–rail interface is one of the most important aspects of railway research, considering the many phenomena involved (wear, adhesion, surface fatigue damage, etc.). For this reason, many scientists have approached the problem mainly by means of theoretical or numerical solutions based on the Hertz's theory, which can be considered the basic starting point for all subsequent research. Pau [13] uses the ultrasonic method to study the wheel rail contact parameters. The principle of the method is to send high-frequency ultrasonic waves (usually in the range 1–20MHz depending on the thickness to test) over the contact interface, evaluating the amount of energy it reflects by calculating the reflection coefficient R = Hi/H0. Where Hi is the amplitude of the ultrasonic wave reflected from the interface subjected to an external load, and H0 is the amplitude measured in the absence of contact. Since engineering surfaces are rough, a contact interface can be figured as a series of parts in contact and voids that act as reflector for the sound energy, due to the fact that only a very minor part of the ultrasounds can be transmitted in gases. Thus, an increase of pressure will result in a reduction of the number and size of these voids and, at the same time, a decrease in the energy reflected from the interface.
The process extremes occur:

- ✓ When the reflection coefficient *R* is 1: in this case no energy is transmitted through the interface (i.e. no contact exists);

- ✓ When the value of R is 0: all the energy is transmitted through the interface, implying that each point of the two surfaces is in (perfect) contact.

In practice the normal load carried on the contact causes both wheel and rail to deform locally to the contact and the load is spread over a contact area or contact patch. For normal railway loads and wheel diameters each contact patches has roughly the size of a finger nail. The wheel cross sectional profile is either coned or a circular arc and the rail head profile is also a circular arc then the load distribution can be calculated analytically and is of the form given by Hertz [12].

If at any time there is a radius in contact with another radius or flat, contact stresses will occur. In the case of two spheres, contacting each other, the entire force will be imparted into a theoretical point. Due to elastic properties of the materials this point will deform to a contact area. The deformation that occurs will produce high tensile and compressive stresses in the materials. Even if a singular loading does not produce a failure, it can lead to future fatigue or surface damage. The maximum pressure within the contact area occurs as a compression in the center. Knowing the maximum pressure then allows you to calculate out the principal stresses along the vertical axis. With the principal stresses and the shear stresses known, evaluations can be made. The first evaluation should be to compare the maximum stresses to the yield or shear strength of the material. The total stresses developed in the rail are the sum of the stresses at the wheel/rail contact (named as Hertz stresses), stresses resulted from rail bending about the ballast, stresses resulted from rail head bending about the web, stresses resulted from thermal effects, and plastic stresses remaining in the rail after the removal of the external load. With the exception of the last two categories all other stresses can be calculated on the assumption of an elastic behavior.

Chapter 3

3. Analysis of Rail-Wheel Surface Contact Geometry

3.1. Introduction

To obtain accurate solutions of the wheel/rail contact problem there are different steps and procedures to be employed. The calculation of wheel-rail contact forces in the dynamic simulation of railroad vehicles involves the following steps[2]:

1. Location of the position of the contact points on the surfaces of the wheel and rail.
2. Calculation of the normal contact forces.
3. Calculation of the tangential (creep) forces and moments.

In this paper the first priority is given to the analysis of wheel/rail surface geometry to locate the accurate positions of contact points. The accuracy of the final solution of wheel/rail contact depends on the accurate prediction of the contact points. The accuracy of the contact point locations depends on the accurate representation of the geometry of wheel and rail surfaces. The wheel/rail contact surface representation can be defined by using:

- ✓ The radii of curvatures (wheel tread surface, rail head surface and track)
- ✓ The tangent vectors of the contact point
- ✓ The normal vectors to the surfaces of the contact point
- ✓ The body coordinate systems (relative coordinate system)
- ✓ The wheel/rail surface parameters (${S_1}^w, {S_2}^w, {S_1}^r, and\ {S_2}^r$)
- ✓ The orientation of rail and the position of wheel

3.2. Analysis of Rail Head Surface Geometry

Rails are longitudinal steel members having different composition and shape depending on the service they are required to perform. Its composition and shape play a great role in its long life service and smooth interaction with wheel to transfer the axle load to sleepers and the ballasts. Kataoka [9] rails are the most fundamentally important members of railways and have the following roles.

(1) They directly support the wheel load with large carriages.

(2) They impart safe and smooth travel surface to carriages and provide safe passage and guidance.

(3) They disperse the wheel load to rail support and facilitate rail track maintenance control. The rail configuration and material are determined in order to fulfill these roles.

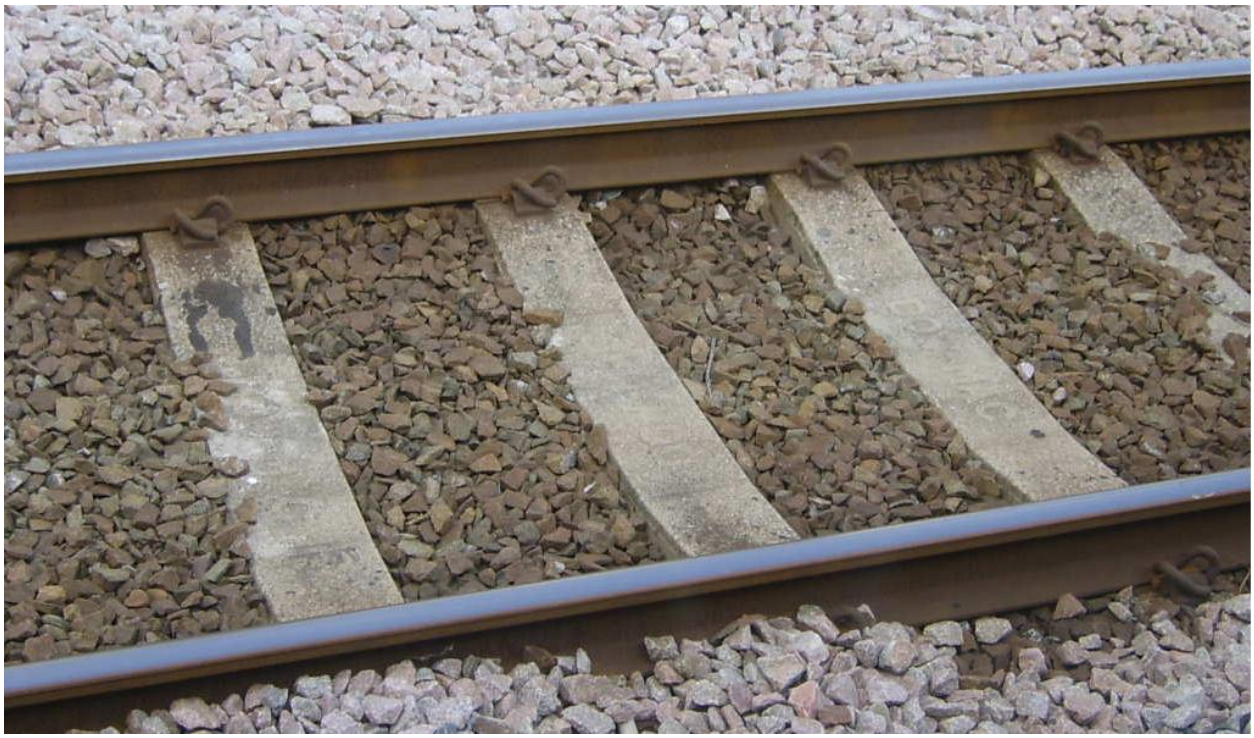

Figure 3.1: Rail arrangements and track components

This section mainly concerns about analyzing the rail head shape and determining the general rail lateral, longitudinal and vertical profile that is used to simply predict the contact points with the wheel profile. It is the first step in the analysis of wheel/rail contact and modeling vehicle dynamics in which the locations of points of contacts between the wheel and the rail are determined. To determine those points of contacts it is necessary to fully define the wheel/rail geometry because the final numerical simulation is dependent on the accuracy of the locations of the contact points and the accuracy of representation of wheel/rail geometry. Escalona [2] the method proposed for the search of the contact points requires the surfaces of the wheel and rail to be mathematically parameterized. The description and representation of rail surface geometry is taken as a general, which is used to represent arbitrary rail profile.

To fully define the rail surface geometry that is it's longitudinal, vertical and cross sectional profile, the global and local coordinate systems are the most appropriate.

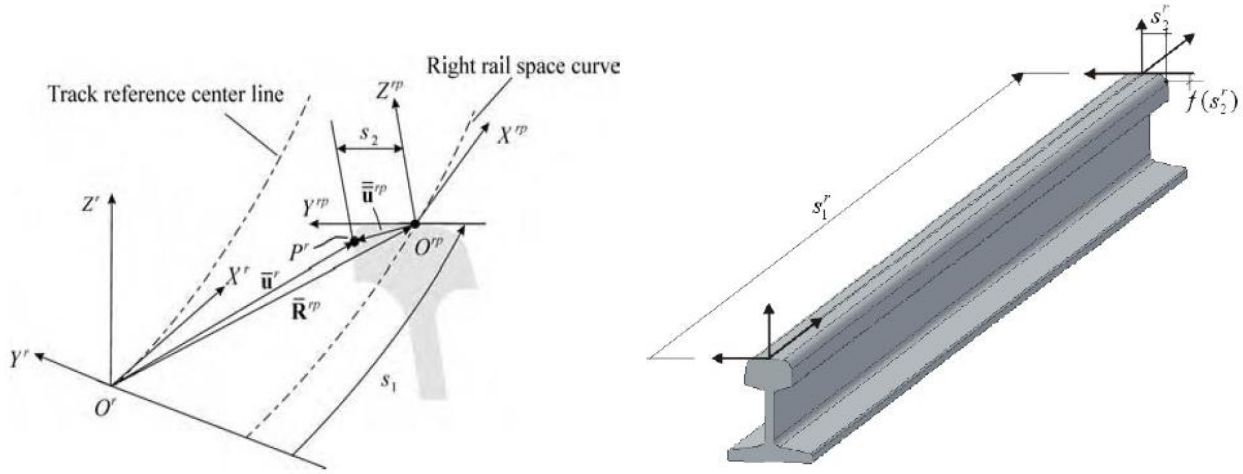

Figure 3.2: Rail cross-sectional and longitudinal profile with profile and global coordinates

Both the right and left rail surfaces will be parameterized by using longitudinal and lateral surface parameters with the aid of those coordinate systems. Matsumura [15], for a given arc-length coordinate S_1 along the rail centerline, the rail profile is determined and the location of contact points can be obtained using the parameter S_2 along the lateral directions.

In this paper for simplicity of geometry during the analysis of rail surface some assumptions are made:

a. No gauge variation (widening) that is the gauge is always constant
b. Uniform rail cross-section
c. No relative rotations of rails

Therefore based on these assumptions it is possible to take either the right or the left rail for rail surface geometry analysis. In this paper all the analysis is taken on the right wheel and right rail. The global coordinate system is assumed to be fixed on the reference center line which is common center line of both right and left rails. The local (profile or body) coordinate system is fixed somewhere on the surface of rail head aligned its origin on the space curve of the given rail. From the figure shown below **P** is the required point (arbitrary point) on the rail head surface. It is determined by the coordinates of a point on the rail space curve and the orientation of a profile coordinate system at this point.

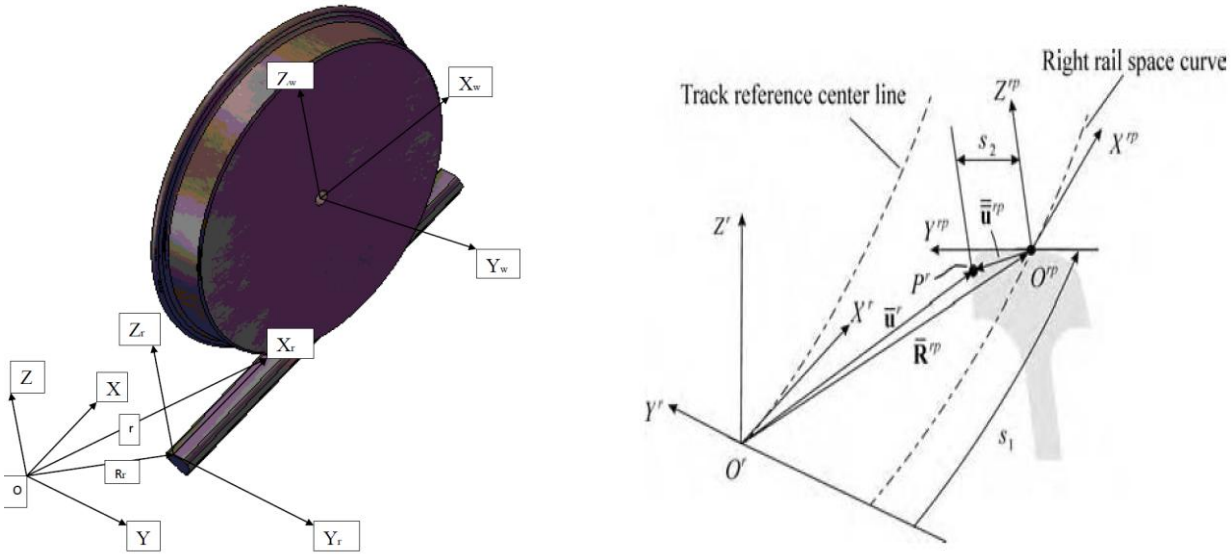

A B

Figure 3.3: Wheel/rail assembly (A) and (B) the location of arbitrary point **P** on the rail head surface

3.2.1. Mathematical Model to Locate Contact Point on the Rail Head Surface

By using the vector addition rule:

$$\overrightarrow{u^r} = \overrightarrow{R^{rp}} + \overrightarrow{A^r}\overrightarrow{u^{rp}} \quad \text{----------3.1}$$

Where,

$\overrightarrow{u^r}$ = The position of arbitrary point on the rail head surface relative to the fixed global coordinate system (X, Y, Z)

$\overrightarrow{R^{rp}}$ = The position of origin of the rail profile coordinate system relative to the fixed global coordinate system

$\overrightarrow{A^r}$ = The rotational transformation matrix used to show the orientation of the rail profile coordinate system relative to the fixed global coordinate system

$\overrightarrow{u^{rp}}$ = The location of the point **P** relative to the profile coordinate system

During the analysis of rail head surface geometry and locating the positions of contact point **P** on the rail head surface there are two commonly used parameters.

1. Rail longitudinal surface parameters ($S_1{}^r$)
2. Rail lateral surface parameters ($S_2{}^r$)

By using these parameters and inserting them into equation (3.1)

$$\overrightarrow{u^r(s_1{}^r, s_2{}^r)} = \overrightarrow{R^{rp}(S_1{}^r)} + \overrightarrow{A^r(S_1{}^r)} \times \overrightarrow{u^{rp}(S_1{}^r, S_2{}^r)} \quad \text{----------3.2}$$

From this equation the position of the arbitrary point **P** on the rail head surface relative to the global coordinate system depends on both longitudinal and lateral surface parameters whereas the position and orientation of the origin of the rail profile frame depends only on the longitudinal surface parameter. When we come to the location of the point **P** relative to the local (body) coordinate system it depends on both parameters depending on the longitudinal rail track shape. If the cross sectional profile of rail is uniform throughout the track the arbitrary point **P** depends only on the lateral surface parameter but if the rail cross section changes along the track it will depends on both lateral and longitudinal surface parameters.

In this research the cross sectional profile of the rail is assumed to be uniform throughout the track. Therefore the location of the point **P** on the rail head surface relative to the profile coordinate system depends only on the lateral surface parameters.

$\overrightarrow{u^r(s_1{}^r, s_2{}^r)} = \overrightarrow{R^{rp}(s_1{}^r)} + \overrightarrow{A(s_1{}^r)} \times \overrightarrow{u^{rp}(s_2{}^r)}$ ----------3.3

Equation (3.3) can be represented in matrix form as follows:

1. The position vector ($\overrightarrow{u^r}$)

   $u^r = \begin{bmatrix} u_x{}^r \\ u_y{}^r \\ u_z{}^r \end{bmatrix}$ The supper script (r) represents the rail, the subscripts x, y, z represents the global position coordinates.

2. The position vector of rail profile coordinate system

   $\overrightarrow{R^{rp}} = \begin{bmatrix} \overrightarrow{R_X{}^{rp}} \\ \overrightarrow{R_Y{}^{rp}} \\ \overrightarrow{R_Z{}^{rp}} \end{bmatrix}$ The supper script (r) represents the rail, the subscripts X, Y, and Z represents the global coordinate system

3. The relative position vector ($\overrightarrow{u^{rp}}$)

   $u^{rp} = \begin{bmatrix} u_x{}^{rp} \\ u_y{}^{rp} \\ u_z{}^{rp} \end{bmatrix}$ The supper script (r) represents the rail, the subscripts x, y, z represents the (body) profile position coordinates.

4. The rotational transformation matrix (A^r)

   To define the orientation of rail profile coordinate system there are four variables applicable in the railroad industries.

- Projection: the projection of the space curve on the horizontal plane (the horizontal tangent plane to the rail head surface)
- Development: the rotation of rail profile frame about Y-axis which is called elevation angle (θ) and it is considered as positive if it advances the increment of Z-axis
- Supper-elevation: the rotation of the rail profile frame about the X-axis (the tangent to space center line curve) ($\emptyset$), it is called the bank angle and it is considered as positive if it results a positive curvature.
- Curvature: the rotation of the rail profile frame about Z-axis (φ), it is the rotation about Z-axis by using the right hand rule.

To determine the rotational transformation matrix of the rail it is better to use the above four variables and the direction cosine method. The orientation and application of the given variables are determined based on the global and profile (body) coordinates systems.

From the direction cosine rule assume that (**i, j and k)** as the unit vectors along the global coordinate system and also (**$\mathbf{i}'$, $\mathbf{j}'$, and $\mathbf{k}'$)** as the unit vectors along the profile coordinate system.

The general rotational transformation matrix with direction cosine method about a single coordinate is calculated based on the successive rotation of the multi-body dynamic object about a given global coordinates. For rail profile coordinates the sequences of rotations are assumed to be about:

Z ⟶ **X** ⟶ **Y (**curve, supper elevation and rolling)**,** all the three successive rotations are assumed to be rotated based on the right hand rule.

$$A_{(\varphi,\emptyset,\theta)} = \begin{bmatrix} i'.i & j'.i & k'.i \\ i'.j & j'.j & k'.j \\ i'.k & j'.k & k'.k \end{bmatrix} \text{----------3.4}$$

1. If the profile coordinate system is rotated about Z axis by an angle φ relative to the global coordinate system, the direction cosines are:

For x' $i'.i = cos\varphi$ For y' $j'.i = -sin\varphi$ For z' $k'.i = 0$

$i'.j = sin\varphi$ $j'.j = cos\varphi$ $k'.j = 0$

$i'.k = 0$ $j'.k = 0$ $k'.k = 1$

$$A_{\varphi} = \begin{bmatrix} cos\varphi & -sin\varphi & 0 \\ sin\varphi & cos\varphi & 0 \\ 0 & 0 & 1 \end{bmatrix} \text{----------3.5}$$

2. Similarly if the profile frame is rotated about X axis by an angle ∅ relative to the global coordinate system

For x' $i'.i = -1$ $i'.j = 0$ $i'.k = 0$ For y' $j'.i = 0$ $j'.j = cos\emptyset$ $j'.k = -sin\emptyset$ For z' $k'.i = 0$ $k'.j = sin\emptyset$ $k'.k = cos\emptyset$

$$A_{\emptyset} = \begin{bmatrix} -1 & 0 & 0 \\ 0 & cos\emptyset & sin\emptyset \\ 0 & -sin\emptyset & cos\emptyset \end{bmatrix} \text{----------3.6}$$

3. If the profile coordinate system is rotated about Y axis again by an angle θ relative to the global coordinate system

For x' $i'.i = cos\theta$ $i'.j = 0$ $i'.k = -sin\theta$ For y' $j'.i = 0$ $j'.j = 1$ $j'.k = 0$ For z' $k'.i = sin\theta$ $k'.j = 0$ $k'.k = cos\theta$

$$A_{\theta} = \begin{bmatrix} cos\theta & 0 & sin\theta \\ 0 & 1 & 0 \\ -sin\theta & 0 & cos\theta \end{bmatrix} \text{----------3.7}$$

Therefore the rotational transformation matrix associated with Z-X-Y, which shows the orientation of the profile coordinate system about the global coordinate system is:

$$A^r = A_{\varphi} A_{\emptyset} A_{\theta} \text{----------3.8}$$

$$A^r = \begin{bmatrix} cos\varphi & -sin\varphi & 0 \\ sin\varphi & cos\varphi & 0 \\ 0 & 0 & 1 \end{bmatrix} \begin{bmatrix} -1 & 0 & 0 \\ 0 & cos\emptyset & sin\emptyset \\ 0 & -sin\emptyset & cos\emptyset \end{bmatrix} \begin{bmatrix} cos\theta & 0 & sin\theta \\ 0 & 1 & 0 \\ -sin\theta & 0 & cos\theta \end{bmatrix} \text{----------3.9}$$

$$A^r = \begin{bmatrix} -cos\varphi & -sin\emptyset cos\varphi & -sin\varphi sin\emptyset \\ -sin\varphi & cos\varphi cos\emptyset & sin\emptyset cos\varphi \\ 0 & -sin\emptyset & cos\emptyset \end{bmatrix} \begin{bmatrix} cos\theta & 0 & sin\theta \\ 0 & 1 & 0 \\ -sin\theta & 0 & cos\theta \end{bmatrix} \text{----------3.10}$$

$$A^r = \begin{bmatrix} -\cos\varphi\cos\theta + \sin\varphi\sin\varphi\sin\theta & -\sin\varphi\cos\emptyset & -\cos\varphi\sin\theta - \sin\varphi\sin\emptyset\cos\theta \\ \sin\varphi\cos\theta + \sin\theta\cos\varphi\sin\emptyset & cos\varphi cos\emptyset & -\sin\varphi\sin\theta + \cos\varphi\sin\emptyset\cos\theta \\ \sin\emptyset\sin\theta & -\sin\emptyset & \cos\emptyset\cos\theta \end{bmatrix} \text{----------3.11}$$

In vector form the position of the contact point on the rail head surface is:

$$\begin{bmatrix} {u_x}^r \\ {u_y}^r \\ {u_z}^r \end{bmatrix} = \begin{bmatrix} \overrightarrow{R_X}^{rp} \\ \overrightarrow{R_Y}^{rp} \\ \overrightarrow{R_Z}^{rp} \end{bmatrix} + \begin{bmatrix} -\cos\varphi\cos\theta + \sin\varphi\sin\varphi\sin\theta & -\sin\varphi\cos\emptyset & -\cos\varphi\sin\theta - \sin\varphi\sin\emptyset\cos\theta \\ \sin\varphi\cos\theta + \sin\theta\cos\varphi\sin\emptyset & cos\varphi cos\emptyset & -\sin\varphi\sin\theta + \cos\varphi\sin\emptyset\cos\theta \\ \sin\emptyset\sin\theta & -\sin\emptyset & \cos\emptyset\cos\theta \end{bmatrix} \begin{bmatrix} {u_x}^{rp} \\ {u_y}^{rp} \\ {u_z}^{rp} \end{bmatrix} \text{----3.12}$$

3.2.2. Mathematical Equations to Calculate the Three Euler Angles

The three input variables sometimes called (Euler angles) are calculated based on the following assumptions:

- ✓ The arc length (s) is projected on the horizontal plane and it is related to the horizontal curvature of the rail space curve as

$$d\varphi = C_H dS \text{ ----------3.13}$$

Where, S is the projected arc length and C_H is the horizontal curvature

$$dS = cos\theta ds \text{ ----------3.14}$$

Where, s is the actual arc length and θ is the development angle

By integrating this equation we can get

$$S = S_0 + (s - s_0)cos\theta \text{ ----------3.15}$$

This is the general equation to represent the projected arc length in terms of the actual arc length

Therefore,

$$d\varphi = C_H cos\theta ds \text{----------3.16}$$

By integrating this equation

$$\varphi = \varphi_0 + \int_{s_0}^{s_1} C_H \, cos\theta ds \text{ ----------3.17}$$

It is not possible to find out solutions throughout the whole rail length by using the above equations since it has different arrangements and orientations which require different input values. Therefore to

simplify these problems it is better to divide the whole rail length into some common segments with the assumption of linearity through each segment. The commonly used railway rail segments are:

- ✓ Tangent segment: zero curvature
- ✓ Curved segment: constant curvature
- ✓ Tangent to curve entry segment: zero curvature on the curve entry and the inverse of radius of curvature at the end of the curve.
- ✓ Curve to tangent entry segment
- ✓ Curve to curve entry segment

In this paper the appropriate segment type selected for the rail surface geometry analysis is the tangent to curve entry segment, which commonly encounter both the horizontal and curvature wheel/rail contact problems. For this segment assume that the bank angle (super-elevation) $\emptyset$ and the horizontal curvature C_H have a linear variation throughout the length of the segment. However the development angle θ is assumed to be equal to zero due to the general assumptions taken from the Hertz contact theory (smooth surface).

$$\emptyset = \frac{\emptyset_1(S-S_0)-\emptyset_0(S-S_1)}{S_1-S_0} \text{ ----------3.18}$$

Similarly,

$$C_H = \frac{C_1(S-S_0)-C_0(S-S_1)}{S_1-S_0} \text{ ----------3.19}$$

Therefore by inserting equation (3.19) into equation (3.17) and integration of the resulting equation the rotation angle about Z axis is:

$$\varphi = \varphi_0 + \frac{1}{S_1-S_0}\left[\frac{C_1}{2}(S-S_0)^2 - \frac{C_0}{2}(S-S_1)^2\right] + \frac{C_0}{2}(S_1-S_0)^2 \text{ ----------3.20}$$

Where, $(C_0, C_1, S_0, and\ S_1)$ are the horizontal curvature and the projected arc length at the entry and exit of the segment respectively. From all the above equations if the value of the actual arc length and the radius of curvature are known all the input variables are simple to be calculated by using the given equations.

If all the four input variables ($S, \theta, \emptyset, and\ \varphi$) are calculated, it would be simple to calculate the coordinates of the contact point by using numerical integration. From the rail rotational transformation matrix equation it is possible to draw the three respective unit vectors, which are sometimes called as unit tangent vectors. The two unit tangent vectors that is along X and Y are the most crucial for the final output of this paper which will be discussed in the coming chapter. The third tangent vector (unit vector along Z axis) is obtained by using the cross-product of the two basic tangent vectors. Therefore the contact point on the rail head surface will be located with the help of x and y profile coordinates. The two unit tangent vectors t_1 and t_2 are taken directly from the first and second columns of the rail rotational transformation matrix.

Along longitudinal rail surface along lateral rail surface

$$t_1{}^r = \begin{bmatrix} -sin\varphi cos\emptyset \\ cos\varphi cos\emptyset \\ -sin\emptyset \end{bmatrix} \qquad t_2{}^r = \begin{bmatrix} -sin\varphi sin\emptyset \\ cos\varphi sin\emptyset \\ cos\emptyset \end{bmatrix} \text{----------3.21}$$

Based on numerical integration $dX(x,y,z)^T = tdS$ where $dX = du^{rp}$ by integrating this equation

Along longitudinal direction Along lateral direction

$$x = x_0 + \int_{S_o{}^r}^{S_1{}^r} -\sin\varphi\cos\emptyset\, ds \qquad x = x_0 + \int_{S_o{}^r}^{S_2{}^r} -\sin\varphi\sin\emptyset ds \text{----------3.22}$$

$$y = y_0 + \int_{S_o{}^r}^{S_1{}^r} \cos\varphi\cos\emptyset ds \qquad y = y_0 + \int_{S_o{}^r}^{S_2{}^r} \cos\varphi\sin\emptyset ds \text{----------3.23}$$

$$z = z_0 + \int_{S_o{}^r}^{S_1{}^r} -\sin\emptyset\, ds \qquad z = z_0 + \int_{S_o{}^r}^{S_2{}^r} \cos\emptyset ds \text{----------3.24}$$

The deviation in the vertical (z) direction is always perpendicular to the plane surface created by the longitudinal and lateral surface parameters.

3.3. Analysis of Wheel Surface Geometry

The dynamic interactions of railway vehicle and rail track depend also on the geometry of railway wheels and wheel set arrangements. In this paper the wheel set is considered as a fixed unit but for simplicity of analysis the assumptions taken for rail geometry analysis are also considered in this section.

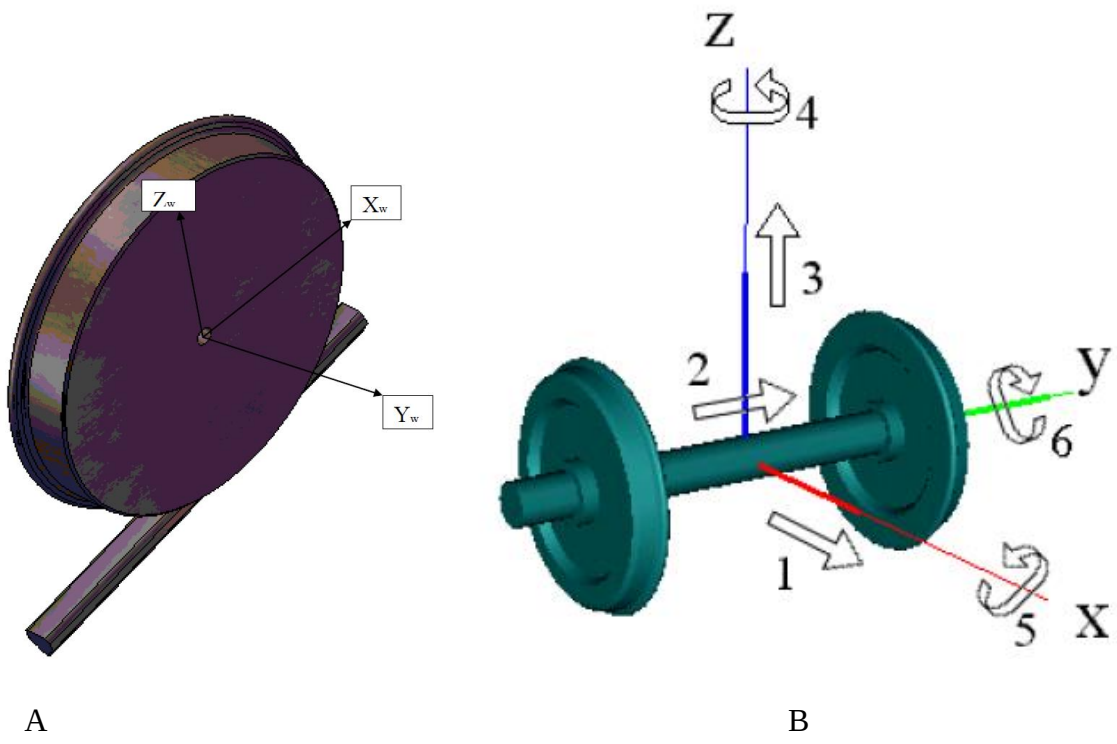

A B

Figure 3.4: Wheel/rail contact (A) and (B) wheel set degree of freedom

Generally the wheel geometry is formed by revolving its symmetrical conic profile about the central axis of the wheel. Its surface geometry can be defined by using the following mathematical modeling with the aid of global and profile (body) coordinate systems similar to the rail head surface geometry. Similarly, it has two surface parameters ($S_1{}^w, S_2{}^w$).

Where, $S_1{}^w$ Represents the lateral surface parameters of the wheel and

$S_2{}^w$ Represents the angular (rotational) surface parameters of the wheel

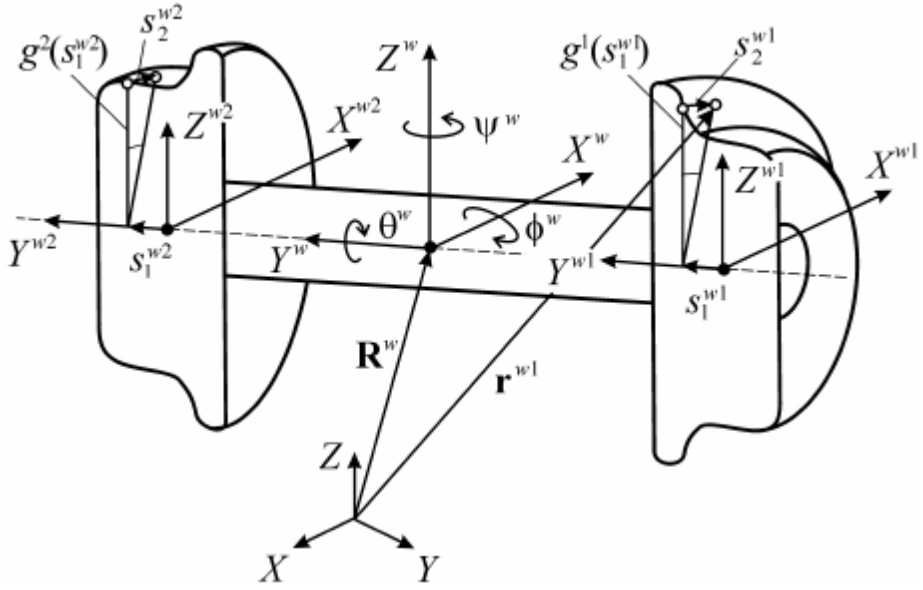

Figure 3.5: Wheel set coordinate systems

Source: (Ryosuke et al), Journal of system design and dynamics, Vol. 5, No. 3, 2011.

3.3.1. Mathematical Model to Locate Contact Point on the Wheel Surface

$$r^w = R^w + A^w u^w \quad \text{----------3.25}$$

By using wheel surface parameters

$$r^w(S_1{}^w, S_2{}^w) = R^w(S_1{}^w) + A^w(S_1{}^w)u^w(S_1{}^w, S_2{}^w) \quad \text{----------3.26}$$

$$u^w = \begin{bmatrix} x^w \\ y^w \\ z^w \end{bmatrix}$$

$$x^w = x_0{}^w + g(s_1{}^w)\sin s_2{}^w$$

$$y^w = -L + s_1{}^w$$

$$z^w = z_0{}^w + g(s_1{}^w)\cos s_2{}^w$$

$g(s_1{}^w)$, is the function that defines the wheel profile

Therefore, for the right wheel the profile position vector is

$$u^w(S_1{}^w, S_2{}^w) = \begin{bmatrix} x_0{}^w + g(s_1{}^w)\sin s_2{}^w \\ -L + s_1{}^w \\ z_0{}^w + g(s_1{}^w)\cos s_2{}^w \end{bmatrix} \text{----------3.27}$$

$$R^w = \begin{bmatrix} R_x{}^w \\ R_y{}^w \\ R_z{}^w \end{bmatrix}$$

To determine the wheel rotational transformation matrix and the position of contact point on the wheel tread surface the following considerations are taken. These are:

1. The sequences of successive rotations

   The wheel profile coordinates successive rotations are assumed to be on the sequences of Y-Z-X (rolling, curve and supper elevation). According to these sequences of rotations:

$$A_{(\varphi,\theta,\emptyset)} = \begin{bmatrix} i'.i & j'.i & k'.i \\ i'.j & j'.j & k'.j \\ i'.k & j'.k & k'.k \end{bmatrix} \text{----------3.28}$$

   ✓ The rotation of the wheel profile about Y axis

For x' $i'.i = cos\theta$ For y' $j'.i = 0$ For z' $k'.i = sin\theta$

$i'.j = 0$ $j'.j = 1$ $k'.j = 0$

$i'.k = -sin\theta$ $j'.k = 0$ $k'.k = cos\theta$

$$A_\theta = \begin{bmatrix} cos\theta & 0 & sin\theta \\ 0 & 1 & 0 \\ -sin\theta & 0 & cos\theta \end{bmatrix} \text{----------3.29}$$

   ✓ The rotation of the wheel profile about Z axis

For x' $i'.i = cos\varphi$ For y' $j'.i = -sin\varphi$ For z' $k'.i = 0$

$i'.j = sin\varphi$ $j'.j = cos\varphi$ $k'.j = 0$

$i'.k = 0$ $j'.k = 0$ $k'.k = 1$

$$A_\varphi = \begin{bmatrix} cos\varphi & -sin\varphi & 0 \\ sin\varphi & cos\varphi & 0 \\ 0 & 0 & 1 \end{bmatrix} \text{----------3.30}$$

   ✓ The rotation of the wheel profile about X axis

For x' $i'.i = -1$ For y' $j'.i = 0$ For z' $k'.i = 0$

$i'.j = 0$ $j'.j = cos\emptyset$ $k'.j = sin\emptyset$

$i'.k = 0$ $j'.k = -sin\emptyset$ $k'.k = cos\emptyset$

$$A_{\emptyset} = \begin{bmatrix} -1 & 0 & 0 \\ 0 & cos\emptyset & sin\emptyset \\ 0 & -sin\emptyset & cos\emptyset \end{bmatrix} \text{----------3.31}$$

$$A^w = A_\theta A_\varphi A_\emptyset$$

$$A^w = \begin{bmatrix} cos\theta & 0 & sin\theta \\ 0 & 1 & 0 \\ -sin\theta & 0 & cos\theta \end{bmatrix} \begin{bmatrix} cos\varphi & -sin\varphi & 0 \\ sin\varphi & cos\varphi & 0 \\ 0 & 0 & 1 \end{bmatrix} \begin{bmatrix} -1 & 0 & 0 \\ 0 & cos\emptyset & sin\emptyset \\ 0 & -sin\emptyset & cos\emptyset \end{bmatrix} \text{----------3.32}$$

$$A^w = \begin{bmatrix} cos\theta & 0 & sin\theta \\ 0 & 1 & 0 \\ -sin\theta & 0 & cos\theta \end{bmatrix} \begin{bmatrix} -cos\varphi & -sin\emptyset cos\varphi & -sin\varphi sin\emptyset \\ -sin\varphi & cos\varphi cos\emptyset & sin\emptyset cos\varphi \\ 0 & -sin\emptyset & cos\emptyset \end{bmatrix} \text{----------3.33}$$

$$\mathrm{A^w} = \begin{bmatrix} -\cos\varphi\cos\theta & -\cos\varphi\sin\emptyset\cos\theta - \sin\emptyset\sin\theta & -\sin\varphi\sin\emptyset\cos\theta + \cos\emptyset\sin\theta \\ -\sin\varphi & cos\varphi cos\emptyset & \cos\varphi\sin\emptyset \\ \cos\varphi\sin\theta & \cos\varphi\sin\emptyset\sin\theta - \sin\emptyset\cos\theta & \sin\varphi\sin\emptyset\sin\theta + \cos\emptyset\cos\theta \end{bmatrix} \text{----------3.34}$$

$$r^w = \begin{bmatrix} {R_x}^w \\ {R_y}^w \\ {R_z}^w \end{bmatrix} + \begin{bmatrix} -\cos\varphi\cos\theta & -\cos\varphi\sin\emptyset\cos\theta - \sin\emptyset\sin\theta & -\sin\varphi\sin\emptyset\cos\theta + \cos\emptyset\sin\theta \\ -\sin\varphi & cos\varphi cos\emptyset & \cos\varphi\sin\emptyset \\ \cos\varphi\sin\theta & \cos\varphi\sin\emptyset\sin\theta - \sin\emptyset\cos\theta & \sin\varphi\sin\emptyset\sin\theta + \cos\emptyset\cos\theta \end{bmatrix} \begin{bmatrix} {x_0}^w + g({s_1}^w)\sin{s_2}^w \\ -L + {s_1}^w \\ {z_0}^w + g({s_1}^w)\cos{s_2}^w \end{bmatrix} \text{---3.35}$$

2. The development angle θ to be zero for smooth wheel surface
   - ✓ The unit tangent vectors at the contact point is obtained by using the formula $dX(x,y,z)^T = tdS$ where $dX = du^w$
   - ✓ Since the wheel profile is dependent on both longitudinal and lateral surface parameters it is impossible to consider the unit vectors separately, instead it is better to derivate u^w with respect to ${s_1}^w and\ {s_2}^w$ to obtain ${t_1}^w and\ {t_2}^w$ respectively.
   - ✓ ${t_1}^w = \frac{d}{d{s_1}^w}(u^w)$ ----------3.36

Therefore, $\frac{d}{d{s_1}^w}(u^w({S_1}^w, {S_2}^w)) = \frac{d}{d{s_1}^w}\begin{bmatrix} {x_0}^w + g({s_1}^w)\sin{s_2}^w \\ -L + {s_1}^w \\ {z_0}^w + g({s_1}^w)\cos{s_2}^w \end{bmatrix}$ ----------3.37

$$t_1{}^w = \begin{bmatrix} \frac{dg(s_1{}^w)}{s_1{}^w}\sin s_2{}^w \\ 1 \\ -\frac{dg(s_1{}^w)}{s_1{}^w}\cos s_2{}^w \end{bmatrix}$$ Along lateral direction ----------3.38

$$\frac{d}{ds_2{}^w}(u^w(S_1{}^w, S_2{}^w)) = \frac{d}{ds_2{}^w}\begin{bmatrix} x_0{}^w + g(s_1{}^w)\sin s_2{}^w \\ -L + s_1{}^w \\ z_0{}^w + g(s_1{}^w)\cos s_2{}^w \end{bmatrix}$$----------3.39

$$t_2{}^w = \begin{bmatrix} g(s_1{}^w)\cos s_2{}^w \\ 1 \\ g(s_1{}^w)\sin s_2{}^w \end{bmatrix}$$ Along longitudinal (rotational) direction ----------3.40

In the case of wheel profile there is no separate representation of X and Y with lateral and longitudinal parameters unlike rail profile due to dependency of wheel parameters on each others. Therefore the lateral and rotational wheel surfaces are defined based on both parameters ($S_1{}^w, S_2{}^w$).

Chapter 4

4. Analysis and Determination of Rail-Wheel Contact Point

4.1. Introduction

Due to the general shape of wheel/rail contacting surface, the railway wheel/rail contact is assumed to be convex contact. Therefore the radii of curvatures for both surfaces will be positive.

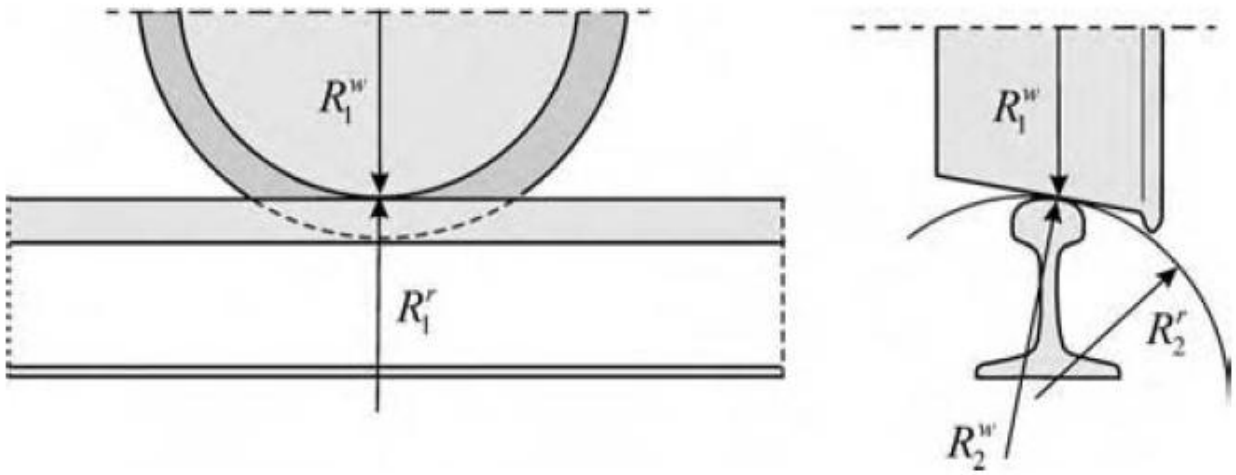

Figure 4.1: Wheel and rail radii of curvatures

Based on those general assumptions, the contact parameters of the two bodies can be defined very well. Some of those contact parameters are:

- ✓ the contact point (area) and dimensions
- ✓ the contact pressure, often called the Hertz's stress
- ✓ the principal stresses (σ_3, σ_2 *and* σ_1)
- ✓ the maximum shear stress

These contact parameters depend on the geometry and shape of the contacting bodies, load and material properties. Based on the Hertz's contact theory and convex form contacting surface of the two bodies, the contact area between them is enveloped by an ellipse.

4.2. Theories of Wheel-Rail Contact

4.2.1. History of Wheel/Rail Contact Mechanics

Knothe [10] studied that history of wheel/rail contact mechanics is an integrated part of contact mechanics. Problems of wheel/rail contact (damage phenomena and influence of contact mechanics on vehicle dynamics, especially on vehicle stability) have been investigated since the middle of the 19th Century. In 1855, Redtenbacher was the first to consider head checking. Stability investigations started with Boedecker (1887) and were continued by Carter (1916); however, they were not recognized at that time. Stability analysis was only considered to be an integrated step in vehicle design in about 1955 when stability problems started to occur in practice. The scientific foundations of our present investigations are Heinrich Hertz, Frederick William Carter and Hans Fromm.

There are two main problems connected with wheel/rail contact mechanics. The first is damage phenomena on the surface of wheel and rail, the second is the running behavior of wheel sets, bogies or railway vehicles on straight track or on curves. Heinrich Hertz was the first to consider these kinds of problems. During his study of wheel/rail contact problem there are some assumptions that he considers. The assumptions of the Hertz's solution are:

- ✓ complete linearity, *i.e.*, linear kinematic equations and linear-elastic material law (additionally the material was isotropic and homogeneous);
- ✓ no friction (Hertz wrote that the surfaces of both bodies had to be completely smooth)
- ✓ both bodies were considered as half-spaces

4.2.2. Wheel-Rail Contact Mechanics Approaches

To analyze the Rail-Wheel contact problem and to find the location of the point of contact there are two broad approaches.

1. Conformal contact approach: In this approach the general assumption is two bodies in contact are closely fitted on the contact region. Therefore in this approach there will be an area contact.
2. Non-conformal contact Approach: If two rigid bodies are under point or line contact the contact between bodies is called non-conformal contact. This approach is used for searching contact points for bodies with different shape and arrangements. Therefore it is applicable to wheel/rail

dynamic interaction to search the point of contact between the rail and the wheel. In this approach there are two commonly used methods.

- ✓ Kinematic Constraint method: In this method it is assumed that there is no consideration of separation and penetration between the rail and wheel contact.
- ✓ Elastic method: This approach is based on the Hertz's contact theory and a compliant force element. In this approach the separation and penetration between wheel and rail contact is considered.

From the two general approaches listed above the second approach (non-conformal contact approach) is mostly applicable to the analysis of wheel/rail contact. This is due to the non-conformal behavior of wheel/rail contact.

To simplify the complexity of the analysis (eliminate the use of langrage multipliers, etc.) and due to the applicability of the Hertz's contact theory to the wheel/rail contact geometry, from the two non-conformal contact searching methods the second method (Elastic Approach) is selected for the analysis and determination of the Wheel/Rail contact point.

In the elastic approach there are some assumptions to be taken based on the Hertz's contact theory.

- ✓ The surfaces of the contacting bodies are continuous and non-conformal
- ✓ The strains are small
- ✓ The stress resulting from the contact force vanishes at a distance far from the contact area.
- ✓ The surfaces are frictionless.
- ✓ The bodies are elastic, and no plastic deformation occurs in the contact area.

4.2.3. Modeling Wheel-Rail Contact

According to this method the location of the contact points can be determined by:

- ✓ Using look-up tables
- ✓ Using discrete nodal search
- ✓ Solving a set of algebraic equations

The first two methods require actual measured data and long and complex analysis, which is time consuming and costly. Therefore for this paper the third method is chosen which is mostly analytical and relatively simple and easily applicable.

To locate the point of contact between wheel and rail surfaces by solving a set of algebraic equations first the following four algebraic equations must be defined well to determine the four parameters that describe the geometry of the wheel and the rail surfaces.

$(t_1{}^r)^T . r^{wr} = 0$ ----------4.1

$(t_2{}^r)^T . r^{wr} = 0$----------4.2

$(t_1{}^w)^T . n^r = 0$----------4.3

$(t_2{}^w)^T . n^r = 0$ ----------4.4

Where

$t_1{}^r,\ t_2{}^r$ Tangents along longitudinal and lateral directions of the rail surfaces respectively

$t_1{}^w, t_2{}^w$ Are tangents along lateral and longitudinal directions of wheel respectively.

$r^{wr}, and\ n^r$ The difference between the wheel and rail position vector and the normal vector of the rail surface respectively

4.2.4. The Position of Contact Point on the Rail Head Surface

From previous chapter we know that:

$u^r = R^{rp} + A^r u^{rp}$ ----------4.5

Assume that $R^{rp} = 0$, then

$u^r = A^r u^{rp}$

u^{rp} -is a function of $s_2{}^r$ therefore, u^{rp} is defined with $t_2{}^r$. If $\theta = 0$ as:

$$t_2{}^r . = \begin{bmatrix} -sin\varphi sin\emptyset \\ cos\varphi sin\emptyset \\ cos\emptyset \end{bmatrix}$$

Therefore,

$$u^{rp}. = \begin{bmatrix} -sin\varphi sin\emptyset {s_2}^r \\ cos\varphi sin\emptyset {s_2}^r \\ cos\emptyset {s_2}^r \end{bmatrix} \text{----------4.6}$$

$$u^r = \begin{bmatrix} -\cos\varphi\cos\theta + \sin\varphi\sin\varphi\sin\theta & -\sin\varphi\cos\emptyset & -\cos\varphi\sin\theta - \sin\varphi\sin\emptyset\cos\theta \\ \sin\varphi\cos\theta + \sin\theta\cos\varphi\sin\emptyset & cos\varphi cos\emptyset & -\sin\varphi\sin\theta + \cos\varphi\sin\emptyset\cos\theta \\ \sin\emptyset\sin\theta & -\sin\emptyset & \cos\emptyset\cos\theta \end{bmatrix} \begin{bmatrix} -sin\varphi sin\emptyset {s_2}^r \\ cos\varphi sin\emptyset {s_2}^r \\ cos\emptyset {s_2}^r \end{bmatrix} \text{----------4.7}$$

For $\theta = 0$

$$A^r = \begin{bmatrix} -\cos\varphi & -\sin\varphi\cos\emptyset & -\sin\varphi\sin\emptyset \\ \sin\varphi & cos\varphi cos\emptyset & \cos\varphi\sin\emptyset \\ 0 & -\sin\emptyset & \cos\emptyset \end{bmatrix} \text{----------4.8}$$

$$\mathrm{u}^r = \begin{bmatrix} -\cos\varphi & -\sin\varphi\cos\emptyset & -\sin\varphi\sin\emptyset \\ \sin\varphi & cos\varphi cos\emptyset & \cos\varphi\sin\emptyset \\ 0 & -\sin\emptyset & \cos\emptyset \end{bmatrix} \begin{bmatrix} -sin\varphi sin\emptyset {s_2}^r \\ cos\varphi sin\emptyset {s_2}^r \\ cos\emptyset {s_2}^r \end{bmatrix} \text{----------4.9}$$

$$u^r = \begin{bmatrix} cos\varphi sin\varphi sin\emptyset({s_2}^r) - cos\varphi sin\varphi cos\emptyset sin\emptyset({s_2}^r) - sin\varphi cos\emptyset sin\emptyset({s_2}^r) \\ -sin^2\varphi sin\emptyset({s_2}^r) + cos^2\varphi cos\emptyset sin\emptyset({s_2}^r) + cos\varphi cos\emptyset sin\emptyset({s_2}^r) \\ -cos\varphi sin^2\emptyset({s_2}^r) + cos^2\emptyset({s_2}^r) \end{bmatrix} \text{----------4.10}$$

Assume that:

$cos\varphi = m$, $sin\varphi = A$, $cos\emptyset = n$ and $sin\emptyset = B$

Therefore,

$$u^r = \begin{bmatrix} mAB({s_2}^r) - mABn({s_2}^r) - ABn({s_2}^r) \\ -A^2B({s_2}^r) + m^2nB({s_2}^r) + mnB({s_2}^r) \\ -mB^2({s_2}^r) + n^2({s_2}^r) \end{bmatrix} \text{----------4.11}$$

4.2.5. The Position of Contact Point on the Wheel Surface

$$r^w = R^w + A^w u^w \text{----------4.12}$$

For $\theta = 0$

$$A^w = \begin{bmatrix} -cos\varphi & -cos\varphi sin\emptyset & -sin\varphi sin\emptyset \\ -sin\varphi & cos\varphi cos\emptyset & cos\varphi sin\emptyset \\ 0 & -sin\emptyset & cos\emptyset \end{bmatrix} \text{----------4.13}$$

Assume:

$x_0, y_0, z_0, and\ R^w = 0$ and $g({s_1}^w) = k$

$$u^w = \begin{bmatrix} ksin(s_2{}^w) \\ -L + s_1{}^w \\ kcos(s_2{}^w) \end{bmatrix} \text{----------4.14}$$

$$r^w = A^w u^w \text{----------4.15}$$

$$r^w = \begin{bmatrix} -cos\varphi & -cos\varphi sin\emptyset & -sin\varphi sin\emptyset \\ -sin\varphi & cos\varphi cos\emptyset & cos\varphi sin\emptyset \\ 0 & -sin\emptyset & cos\emptyset \end{bmatrix} \begin{bmatrix} ksin(s_2{}^w) \\ -L + s_1{}^w \\ kcos(s_2{}^w) \end{bmatrix} \text{----------4.16}$$

$$r^w = \begin{bmatrix} -kcos\varphi sin(s_2{}^w) - cos\varphi sin\emptyset(s_1{}^w - L) - ksin\varphi sin\emptyset cos(s_2{}^w) \\ -ksin\varphi \sin(s_2{}^w) + cos\varphi cos\emptyset(s_1{}^w - l) + kcos\varphi sin\emptyset cos(s_2{}^w) \\ -sin\emptyset(s_1{}^w - l) + kcos\emptyset cos(s_2{}^w) \end{bmatrix} \text{----------4.17}$$

$$r^w = \begin{bmatrix} -kmsin(s_2{}^w) - mB(s_1{}^w - L) - kABcos(s_2{}^w) \\ -kAsin(s_2{}^w) + mn(s_2{}^w - L) + kmBcos(s_2{}^w) \\ -B(s_1{}^w - L) + kncos(s_2{}^w) \end{bmatrix} \text{----------4.18}$$

4.2.6. The Position of Wheel/Rail Contact Points

$$r^{wr} = r^w - u^r \text{----------4.19}$$

$$r^{wr} = \begin{bmatrix} -\mathrm{kmsin(s_2{}^w) - mB(s_1{}^w - L) - kABcos(s_2{}^w)} \\ -\mathrm{kAsin(s_2{}^w) + mn(s_2{}^w - L) + kmBcos(s_2{}^w)} \\ -\mathrm{B(s_1{}^w - L) + kncos(s_2{}^w)} \end{bmatrix} - \begin{bmatrix} \mathrm{mAB(s_2{}^r) - mABn(s_2{}^r) - ABn(s_2{}^r)} \\ \mathrm{-A^2B(s_2{}^r) + m^2nB(s_2{}^r) + mnB(s_2{}^r)} \\ \mathrm{-mB^2(s_2{}^r) + n^2(s_2{}^r)} \end{bmatrix} \text{--------4.20}$$

$$r^{wr} = \begin{bmatrix} \mathrm{-kmsin(s_2{}^w) - mB(s_1{}^w - L) - kABcos(s_2{}^w) - mAB(s_2{}^r) + mABn(s_2{}^r) + ABn(s_2{}^r)} \\ \mathrm{-kAsin(s_2{}^w) + mn(s_2{}^w - L) + kmBcos(s_2{}^w) + A^2B(s_2{}^r) - m^2nB(s_2{}^r) - mnB(s_2{}^r)} \\ \mathrm{-B(s_1{}^w - L) + kncos(s_2{}^w) + mB^2(s_2{}^r) - n^2(s_2{}^r)} \end{bmatrix} \text{----------4.21}$$

4.2.7. Searching Solutions for Wheel/Rail Contact Parameters

✓ $(t_1{}^r)^T . r^{wr} = 0$ ----------4.22

$$t_1{}^r = \begin{bmatrix} -sin\varphi cos\emptyset \\ cos\varphi cos\emptyset \\ -sin\emptyset \end{bmatrix} = \begin{bmatrix} -An \\ mn \\ -B \end{bmatrix}$$

$$\begin{bmatrix} -An \\ mn \\ -B \end{bmatrix}^T \begin{bmatrix} -\mathrm{kmsin}(s_2{}^{\mathrm{w}}) - \mathrm{mB}(s_1{}^{\mathrm{w}} - \mathrm{L}) - \mathrm{kABcos}(s_2{}^{\mathrm{w}}) - \mathrm{mAB}(s_2{}^{\mathrm{r}}) + \mathrm{mABn}(s_2{}^{\mathrm{r}}) + \mathrm{ABn}(s_2{}^{\mathrm{r}}) \\ -\mathrm{kAsin}(s_2{}^{\mathrm{w}}) + \mathrm{mn}(s_2{}^{\mathrm{w}} - \mathrm{L}) + \mathrm{kmBcos}(s_2{}^{\mathrm{w}}) + \mathrm{A}^2\mathrm{B}(s_2{}^{\mathrm{r}}) - \mathrm{m}^2\mathrm{nB}(s_2{}^{\mathrm{r}}) - \mathrm{mnB}(s_2{}^{\mathrm{r}}) \\ -\mathrm{B}(s_1{}^{\mathrm{w}} - \mathrm{L}) + \mathrm{kncos}(s_2{}^{\mathrm{w}}) + \mathrm{mB}^2(s_2{}^{\mathrm{r}}) - \mathrm{n}^2(s_2{}^{\mathrm{r}}) \end{bmatrix} = 0 \text{----------4.23}$$

$$(\mathrm{A}^2\mathrm{Bn} + \mathrm{m}^2\mathrm{nB} - \mathrm{Bn})\mathrm{kcos}(s_2{}^{\mathrm{w}}) + (\mathrm{ABmn} + \mathrm{m}^2\mathrm{n}^2 + \mathrm{B}^2)s_1{}^{\mathrm{w}} + (\mathrm{A}^2\mathrm{B} - \mathrm{A}^2\mathrm{m}^2\mathrm{Bn} - \mathrm{A}^2\mathrm{n}^2\mathrm{B} + \mathrm{A}^2\mathrm{Bmn} - \mathrm{m}^3\mathrm{n}^2\mathrm{B} - \mathrm{m}^2\mathrm{n}^2\mathrm{B} - \mathrm{mB}^3 - \mathrm{Bn}^2)s_2{}^{\mathrm{r}} = \mathrm{L}(\mathrm{ABmn} + \mathrm{m}^2\mathrm{n}^2 + \mathrm{B}^2)$$

$$(t_2{}^r)^T . r^{wr} = 0 \text{----------4.24}$$

$$t_2{}^r = \begin{bmatrix} -sin\varphi sin\emptyset \\ cos\varphi sin\emptyset \\ cos\emptyset \end{bmatrix} = \begin{bmatrix} -AB \\ mB \\ n \end{bmatrix}$$

$$\begin{bmatrix} -AB \\ mB \\ n \end{bmatrix}^T \begin{bmatrix} -\mathrm{kmsin}(s_2{}^{\mathrm{w}}) - \mathrm{mB}(s_1{}^{\mathrm{w}} - \mathrm{L}) - \mathrm{kABcos}(s_2{}^{\mathrm{w}}) - \mathrm{mAB}(s_2{}^{\mathrm{r}}) + \mathrm{mABn}(s_2{}^{\mathrm{r}}) + \mathrm{ABn}(s_2{}^{\mathrm{r}}) \\ -\mathrm{kAsin}(s_2{}^{\mathrm{w}}) + \mathrm{mn}(s_2{}^{\mathrm{w}} - \mathrm{L}) + \mathrm{kmBcos}(s_2{}^{\mathrm{w}}) + \mathrm{A}^2\mathrm{B}(s_2{}^{\mathrm{r}}) - \mathrm{m}^2\mathrm{nB}(s_2{}^{\mathrm{r}}) - \mathrm{mnB}(s_2{}^{\mathrm{r}}) \\ -\mathrm{B}(s_1{}^{\mathrm{w}} - \mathrm{L}) + \mathrm{kncos}(s_2{}^{\mathrm{w}}) + \mathrm{mB}^2(s_2{}^{\mathrm{r}}) - \mathrm{n}^2(s_2{}^{\mathrm{r}}) \end{bmatrix} = 0 \text{----------4.25}$$

$$\mathrm{K}(\mathrm{A}^2\mathrm{B}^2 + \mathrm{m}^2\mathrm{B}^2 + \mathrm{n}^2)\mathrm{cosS}_2{}^{\mathrm{w}} + (\mathrm{mAB}^2 + \mathrm{m}^2\mathrm{nB} - \mathrm{nB})\mathrm{S}_1{}^{\mathrm{w}} + (2\mathrm{mA}^2\mathrm{B}^2 - \mathrm{A}^2\mathrm{B}^2\mathrm{nm} - \mathrm{m}^3\mathrm{B}^2\mathrm{n} - \mathrm{m}^2\mathrm{B}^2\mathrm{n} + \mathrm{B}^2\mathrm{mn} + \mathrm{n}^3)\mathrm{S}_2{}^{\mathrm{r}} = \mathrm{L}(\mathrm{AB}^2\mathrm{m} + \mathrm{m}^2\mathrm{nB} - \mathrm{nB})$$

✓ $(t_2{}^r)^T . n^w = 0$----------4.26

$$\begin{bmatrix} -AB \\ mB \\ n \end{bmatrix}^T \begin{bmatrix} ksins_2{}^w \\ -k(\frac{dk}{ds_1{}^w}) \\ -kcoss_2{}^w \end{bmatrix} = 0$$

$$-kABsin(s_2{}^w) - kBm\frac{dk}{ds_1{}^w} - nkcos(s_2{}^w) = 0 \text{ ----------4.27}$$

From this equation $\frac{dk}{ds_1{}^w}$ is some differential equation which is not compatible with the other linear equation. Therefore it needs to be represented by other linear equations.

✓ $(t_1{}^r)^T . n^w = 0$----------4.28

$$\begin{bmatrix} -An \\ mn \\ -B \end{bmatrix}^T \begin{bmatrix} ksins_2{}^w \\ -k(\frac{dk}{ds_1{}^w}) \\ -kcoss_2{}^w \end{bmatrix} = 0$$

From this equation

$$\frac{dk}{ds_1{}^w} = \frac{B}{mn}\cos(s_2{}^w) - \frac{A}{m}sin(s_2{}^w) \text{ ----------4.29}$$

By inserting equation (4.29) in to equation (4.27) we can get

$$-\left(k\frac{B^2}{n}+nk\right)\cos(s_2{}^w)=0$$

Therefore the three simultaneous equations are

1. $(A^2Bn+m^2nB-Bn)k\cos(s_2{}^w)+(ABmn+m^2n^2+B^2)s_1{}^w+$
$(A^2B-A^2m^2Bn-A^2n^2B+A^2Bmn-m^3n^2B-m^2n^2B-mB^3-Bn^2)s_2{}^r=L(ABmn+m^2n^2+B^2)$

2. $K(A^2B^2+m^2B^2+n^2)\cos s_2{}^w+(mAB^2+m^2nB-nB)s_1{}^w+$
$(2mA^2B^2-A^2B^2nm-m^3B^2n-m^2B^2n+B^2mn+n^3)\,s_2{}^r=L(AB^2m+m^2nB-nB)$

3. $-\left(k\frac{B^2}{n}+nk\right)\cos(s_2{}^w)=0$

By solving these equations simultaneously:

$\cos(s_2{}^w)=0$----------4.30

This implies that $s_2{}^w=90^\circ \text{ or } 270^\circ$

Assume that

$(mAB^2+m^2Bn-Bn)=a_2$

$L(ABmn+m^2n^2+B^2)=p_2$

$ABmn+m^2n^2+B^2=b_2$

$L(AB^2m+Bm^2n-Bn)=p_1$

$(A^2B-A^2Bm^2n-A^2Bn^2+A^2Bmn-m^3n^2B-m^2n^2B-B^3m-n^2B)=b_3$

$2mA^2B^2-A^2b^2mn-A^2B^2n-m^3B^2n-m^2B^2n+B^2mn+n^3=a_3$

Therefore:

$s_2{}^r=\frac{a_2p_2-b_2p_1}{a_2b_3-a_3b_2}$ ----------4.31

From this equation by using distribution and elimination method

$a_2p_2-b_2p_1=0$

$a_2 b_3 - a_3 b_2 \neq 0$

This implies that:

$s_2{}^r = 0$ ----------4.32

On the other hand,

$s_1{}^w = \frac{p_1(a_2 b_3 + a_3 b_2) - (p_1 b_2 a_3 + a_3 a_2 p_2)}{a_2(a_2 b_3 - a_3 b_2)}$----------4.33

4.3. Analysis of Load Distribution and Contact Point Shape

If two elastic nonconforming bodies contact together then according to the Hertz contact theory, the contact area is elliptical in shape with a major semi-axis **a** and a minor semi-axis **b** [17]. The distribution of the contact pressure in this elliptical area represents a semi-ellipsoid, which can be expressed as:

$$P = \frac{3F_n}{2\pi ab}\sqrt{1 - \left(\frac{x}{a}\right)^2 - \left(\frac{y}{b}\right)^2}$$ ----------4.34

Based on the Hertz contact theory, the contact point is very small relative to the overall dimension of railway wheel and rail surfaces. This very small contact point has elliptical shape.

From the above formula **a** and **b** are semi axes of the contact ellipse whereas X and Y are the required coordinates to specify the point of contacts on the rail surface based on the lateral rail surface parameter.

The contact ellipse semi-axes a and b are determined as follows:

$a = \mathbf{m}(3\pi F_n(K_w + K_r)/4K_3)^{1/3}$----------4.35

$b = \mathbf{n}(3\pi F_n(K_w + K_r)/4K_3)^{1/3}$ ----------4.36

m and **n** are Hertz coefficients and they are given as a function of the angle θ $(0^0 - 180^0)$

$\theta = cos^{-1}\left(\frac{K_4}{K_3}\right)$

K_w, and K_r are constants that depend on the material properties of railway wheel and rail respectively.

Where

$K_w = \frac{1-(v^w)^2}{\pi E^w}$ v^w, and E^w are Poisson's ratio and young's modulus of the railway wheel material

$K_r = \frac{1-(v^r)^2}{\pi E^r}$ v^r, and E^r are Poisson's ratio and young's modulus of railway rail material

Whereas K_3 depends on the geometric properties of the two bodies

$$K_3 = A + B = \frac{1}{2}\left(\frac{1}{{R_1}^w} + \frac{1}{{R_2}^w} + \frac{1}{{R_1}^r} + \frac{1}{{R_2}^r}\right) \text{----------4.37}$$

$$K_4 = B - A = \frac{1}{2}\sqrt{\left(\frac{1}{{R_1}^w} - \frac{1}{{R_2}^w}\right)^2 + \left(\frac{1}{{R_1}^r} - \frac{1}{{R_2}^r}\right)^2 + 2\left(\frac{1}{{R_1}^w} - \frac{1}{{R_2}^w}\right)\left(\frac{1}{{R_1}^r} - \frac{1}{{R_2}^r}\right)cos2\varphi} \text{----------4.38}$$

${R_1}^w and\ {R_1}^r$, are the principal rolling radii of the wheel and the rail respectively

${R_2}^w and\ {R_2}^r$, are the principal transverse radii of curvature of the wheel and rail respectively

The direction of the axes of the contact ellipse can be determined based on the radii of curvature and the rolling radii for the two bodies in contact.

If $\frac{1}{{R_1}^w} + \frac{1}{{R_1}^r} \geq \frac{1}{{R_2}^w} + \frac{1}{{R_2}^r}$, the transverse semi axis of the contact ellipse (y direction) is greater than or equal to the longitudinal semi-axis.

If $\frac{1}{{R_1}^w} + \frac{1}{{R_1}^r} \leq \frac{1}{{R_2}^w} + \frac{1}{{R_2}^r}$, the transverse semi axis of the contact ellipse (y direction) is less than or equal to the longitudinal semi-axis

Chapter 5

5. Simulation of Wheel/Rail Contact

5.1. Material Selection

5.1.1. Rail Material Selection

Rails are grouped according to their standards, strength, grade, quality and length. The rail steel qualities can be distinguished in to two categories.

- ✓ Normal steel quality, with an ultimate tensile strength of 700-900 MPa
- ✓ Hard steel quality, used mainly on curves, and crossings etc. with an ultimate tensile strength of 900-1200 MPa

Concerning their chemical compositions rails have great varieties of carbon, manganese, chromium and silicon contents depending on their requirements. Since the rails have to withstand the impact load, friction and stress of freights, they should have sufficient strength, hardness, toughness and good welding performance. However a large increase in rail mechanical strength may result brittle failure and as a result a further increase is not desirable. Similarly, the same material property is selected for wheel materials.

Table 5.1: Rail Material Selection

S.N	Radii of curvature (mm)	Gauge (mm)	Axle load (N)	UIC Standard (Kg)	Poison's Ratio	ANSYS structural Element type	Young's Modulus (GPa)
1	$R_1{}^r = \infty$	1435	25000	54	0.3	8 node-Solid 185	207
2	$R_2{}^r = 300$						

Source: Ethiopian Railway Corporation and UIC rail standards

5.1.2. Wheel Material Selection

Table 5.2: Wheel Material Selection

S.N	Radii of curvature (mm)	Gauge (mm)	Axle load (N)	UIC Standard (Kg)	Poison's Ratio	ANSYS structural Element type	Young's Modulus (GPa)
1	$R_1{}^w = 420$	1435	25000	64	0.3	8 node-Solid 185	207
2	$R_2{}^w = \infty$						

Source: Ethiopian Railway Corporation and UIC wheel standards

5.2. Conditions of Wheel/Rail Contact Simulations

The general conditions considered during the wheel rail contact simulation are the assumption of the Hertz contact theory. As explained in the previous chapter the common Hertz assumptions are:

- ✓ Isotropic and homogenous material
- ✓ no friction (Hertz wrote that the surfaces of both bodies had to be completely smooth)
- ✓ both bodies were considered as half-spaces
- ✓ The contact is elastic

According to these assumptions and analytical results obtained in chapter 4 of equation (4.32), at which, $s_2{}^r = 0$, and by using equation (4.34) the maximum pressure (Hertz stress) occur on the centerline of the rail head.

$$P = \frac{3F_n}{2\pi ab}\sqrt{1 - \left(\frac{x}{a}\right)^2 - \left(\frac{y}{b}\right)^2}$$

If x=0 and y=0 that is if the point of contact is on the centerline of the rail head the stress is maximum, which is equal to:

$$P = \frac{3F_n}{2\pi ab} \text{ ---------- (5.1)}$$

Depending on the size and orientation of the contact ellipse the positions of the contact point may be shifted in different directions based on the magnitude of x or y. However, based on the above general Hertz contact formula and assumptions, the stress due to wheel/rail contact decreases and becomes zero if it goes far away from the centerline of the rail head. Similarly, the wheel/rail contact stress is inversely proportional to the major and minor axis of the contact ellipse.

5.3. Analytical Results

On the center of rail head the contact pressure (stress) is equal to:

$P = \frac{3F_n}{2\pi ab}$, $a = \mathbf{m}(3\pi F_n(K_w + K_r)/4K_3)^{1/3}$ and $b = \mathbf{n}(3\pi F_n(K_w + K_r)/4K_3)^{1/3}$

Where,

$K_w = \frac{1-(v^w)^2}{\pi E^w}$, $K_w = \frac{1-(0.3)^2}{\pi \times 207 \times 10^9 N/m^2} = 1.4 \times 10^{-12} \frac{m^2}{N}$

$K_r = \frac{1-(v^r)^2}{\pi E^r} = \frac{1-(0.3)^2}{\pi \times 207 \times 10^9 N/m^2} = 1.4 \times 10^{-12} \frac{m^2}{N}$

$K_3 = A + B = \frac{1}{2}\left(\frac{1}{{R_1}^w} + \frac{1}{{R_2}^w} + \frac{1}{{R_1}^r} + \frac{1}{{R_2}^r}\right)$, $K_3 = \frac{1}{2}\left(\frac{1}{420mm} + \frac{1}{\infty} + \frac{1}{\infty} + \frac{1}{300mm}\right)$

$K_3 = 0.00286/mm$

$$K_4 = B - A = \frac{1}{2}\sqrt{\left(\frac{1}{{R_1}^w} - \frac{1}{{R_2}^w}\right)^2 + \left(\frac{1}{{R_1}^r} - \frac{1}{{R_2}^r}\right)^2 + 2\left(\frac{1}{{R_1}^w} - \frac{1}{{R_2}^w}\right)\left(\frac{1}{{R_1}^r} - \frac{1}{{R_2}^r}\right)cos2\varphi}$$

- ✓ For a straight segment the curvature of the rail is zero.

$\varphi = 0^\circ$

$${K_4}^0 = \frac{1}{2}\sqrt{\left(\frac{1}{420} - \frac{1}{\infty}\right)^2 + \left(\frac{1}{\infty} - \frac{1}{300}\right)^2 + 2\left(\frac{1}{420} - \frac{1}{\infty}\right)\left(\frac{1}{\infty} - \frac{1}{300}\right)cos2(0^\circ)}$$

${K_4}^0 = 4.76 \times 10^{-4}/mm$

- ✓ For a curved segment the curvature of the rail is:

$C_H = \frac{C_1(S-S_0) - C_0(S-S_1)}{S_1 - S_0}$

For 54Kg/m rail block $S_o = 0, S_1 = 1m$ and at the end $S_1 = S$. The curvature $C_0 = 0$ and C_1 is equal to the inverse of the radius of curvature. For the railway vehicle the maximum radius of curvature of the rail is infinity and the standard minimum radius of curvature is 300m. Therefore,

$C_1 = \frac{1}{300m} = 0.0033/m$

$C_H = \frac{C_1(S-S_0) - C_0(S-S_1)}{S_1 - S_0} = \frac{0.0033\,(1-0) - 0}{1-0} = 0.0033/m$

$$\varphi = \varphi_0 + \frac{1}{S_1 - S_0}\left[\frac{C_1}{2}(S - S_0)^2 - \frac{C_0}{2}(S - S_1)^2\right] + \frac{C_0}{2}(S_1 - S_0)^2$$

$$\varphi = 0.0033(0.5) = 0.00165 \text{ rad}$$

$$\varphi = 0.00165 \times \frac{180^\circ}{\pi} = 0.0945^\circ$$

$$K_4 = \frac{1}{2}\sqrt{\left(\frac{1}{420} - \frac{1}{\infty}\right)^2 + \left(\frac{1}{\infty} - \frac{1}{300}\right)^2 + 2\left(\frac{1}{420} - \frac{1}{\infty}\right)\left(\frac{1}{\infty} - \frac{1}{300}\right) cos2(0.0945^\circ)}$$

$$K_4 = 4.77 \times 10^{-4}/mm$$

1. For a straight rail segment.

$$\theta = cos^{-1}\left(\frac{{K_4}^0}{K_3}\right)$$

$$= \cos^{-1}\left(\frac{4.76 \times 10^{-4}}{0.00286}\right) = 80.4^\circ$$

2. For curved rail segment

$$\theta = cos^{-1}\left(\frac{K_4}{K_3}\right) = \cos^{-1}\left(\frac{4.77 \times 10^{-4}}{0.00286}\right) = 80.39^\circ$$

Therefore from the above analytical results the value of theta on the curved and straight rail segment is equal that is no need of separate analysis. By using the following table (the Hertz coefficient) and linear interpolation method the value of m and n for the chosen rail can be easily obtained.

$$\theta_1 = 80^\circ, m_1 = 1.128, n_1 = 0.893, \theta_2 = 85^\circ, m_2 = 1.061, n_2 = 0.944$$

$$\mathbf{m} = \mathbf{m_1} + \frac{m_2 - m_1}{\theta_2 - \theta_1}(\theta - \theta_1)$$

$$\mathbf{m} = 1.128 + \frac{1.061 - 1.128}{85 - 80}(80.4 - 80)$$

$$\mathbf{m} = 1.123$$

$$\mathbf{n} = \mathbf{n_1} + \frac{n_2 - n_1}{\theta_2 - \theta_1}(\theta - \theta_1)$$

$$\mathbf{n} = 0.893 + \frac{0.944-0.893}{85-80}(80.4-80)$$

$$\mathbf{n} = 0.897$$

$$a = m(3\pi F_n(K_w + K_r)/4K_3)^{1/3}$$

$$a = 1.123(3 \times \pi \times \frac{25000\,N\left(2\times1.4\times10^{-12}\frac{m^2}{N}\right)}{4\times\frac{2.86}{m}})^{1/3}$$

$$a = 0.00434\,m$$

$$b = n(3\pi F_n(K_w + K_r)/4K_3)^{1/3}$$

$$b = 0.897 \times (3 \times \pi \times \frac{25000\,N\left(2\times1.4\times10^{-12}\frac{m^2}{N}\right)}{4\times\frac{2.86}{m}})^{1/3}$$

$$b = 0.00346\,m$$

By using the values of a and b, the Hertz stress (contact pressure) will be:

$$\mathrm{P} = \frac{3\mathrm{F_n}}{2\pi\mathrm{ab}} = \frac{3\times25000\,\mathrm{N}}{2\times\pi\times0.00434\ m\times0.00346\ m}$$

$$P = 794.9\,MPa$$

Table 5.3 Hertz coefficients

θ(deg)	**m**	**n**	θ(deg)	**m**	**n**	θ(deg)	**m**	**n**
0.5	61.4	0.1018	10	6.604	0.3112	60	1.486	0.717
1	36.89	0.1314	20	3.813	0.4125	65	1.378	0.759
1.5	27.48	0.1522	30	2.731	0.493	70	1.284	0.802
2	22.26	0.1691	35	2.397	0.530	75	1.202	0.846
3	16.5	0.1964	40	2.136	0.567	80	1.128	0.893
4	13.31	0.2188	45	1.926	0.604	85	1.061	0.944
6	9.79	0.2552	50	1.754	0.641	90	1.0	1.0
8	7.86	0.285	55	1.611	0.678			

Source: Railroad vehicle dynamics: A computational approach (2008)

To determine the size of the contact area, determination of the orientation of the shape of the contact ellipse is necessary. By using some stated formulas in the previous chapter (chapter 4):

$$\frac{1}{{R_1}^w} + \frac{1}{{R_1}^r} \geq \frac{1}{{R_2}^w} + \frac{1}{{R_2}^r}$$

$$\frac{1}{420} + \frac{1}{\infty} \leq \frac{1}{\infty} + \frac{1}{300}$$

Therefore, the transverse semi axis of the contact ellipse (y direction) is less than or equal to the longitudinal semi-axis. The contact ellipse major axis $a = m(3\pi F_n(K_w + K_r)/4K_3)^{1/3}$ is along the length of the rail and the contact ellipse minor axis $b = n(3\pi F_n(K_w + K_r)/4K_3)^{1/3}$ is along the width of the rail.

5.4. Wheel/Rail Contact Simulation with ANSYS (13)

5.4.1. Principal and Shear Stresses

According to Hertz contact theory, on the point of contact the maximum principal stress is perpendicular to the plane of contact point, which is on the line of applied load. The applied load can be either compressive or tensile. The remaining principal stresses are equal. The figure below shows that the load applied due to body (A) on body (B) results the stresses indicated on the figure. In the case of contact point stress, the maximum stress is the third principal stress.

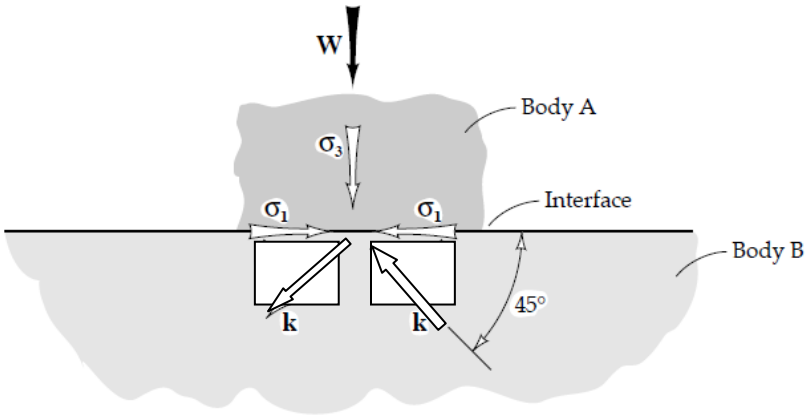

Figure 5.1: Stress status in point contact; σ1, and σ 3 are the principal stresses, and **k** is the shear yield stress of the material

Where,

$$\sigma_1 = \sigma_2 = \sigma_x = \sigma_y = -p_{max}\left[\left(1 - \left|\frac{z}{a}\right| \times atan\left(\frac{1}{\left|\frac{z}{a}\right|}\right)\right) \times (1+v) - \frac{1}{2\times\left(1+\frac{z^2}{a^2}\right)}\right] \text{---------- (5.2)}$$

$$\sigma_3 = \sigma_z = \frac{-p_{max}}{\left(1+\frac{z^2}{a^2}\right)} \text{---------- (5.3)}$$

Assume $z = 0.5 \times a$

In the case of shear stress, on the point of contact where the principal stresses are maximum it is approximately zero and it is maximum on a plane oriented at 45° from the plane of contact (see figure 5.1).

5.4.2. Material Types and Models for ANSYS Simulation

Simulation of wheel/rail contact is based on node-node contact approach because analytical results and mathematical models of wheel and rail contact geometry show that the contact between them is point contact. Therefore, for this kind of contact there are no other approaches producing appropriate results compared to node-node contact approach.

The material properties and element type selected for both wheel and rail materials are similar.

- ✓ Material model

  STRUCTURAL------ELASTIC----ISOTROPIC

- ✓ Element type

  STRUCTURAL----8 NODE-SOLID 185

SOLID185 is used for 3-D modeling of solid structures. It is defined by eight nodes having three degrees of freedom at each node: translations in the nodal x, y, and z directions. The element has plasticity, hyper elasticity, stress stiffening, creep, large deflection, and large strain capabilities.

Pressures may be input as surface loads on the element faces as shown by the circled numbers in the Figure below.

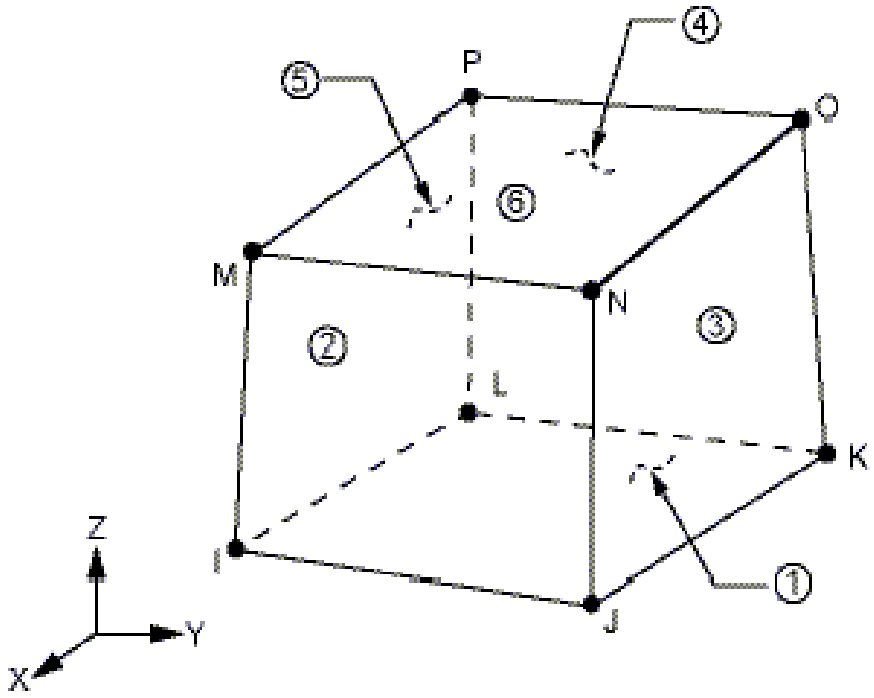

Figure 5.2: Solid 185 element general structures

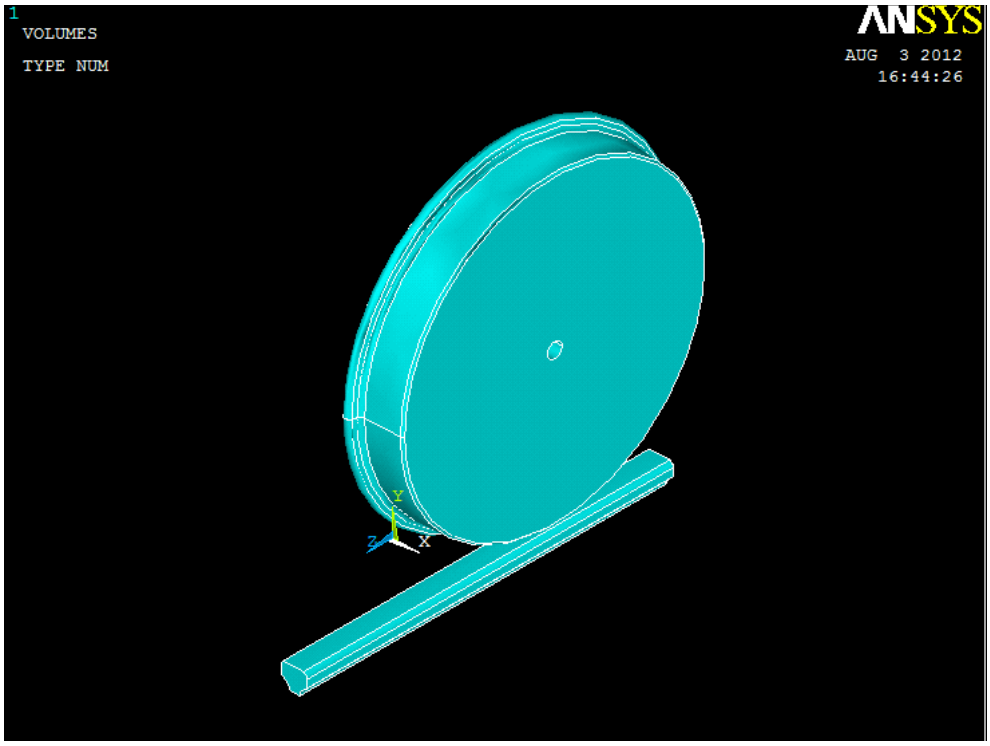

Figure 5.3: Wheel/rail contact model with ANSYS

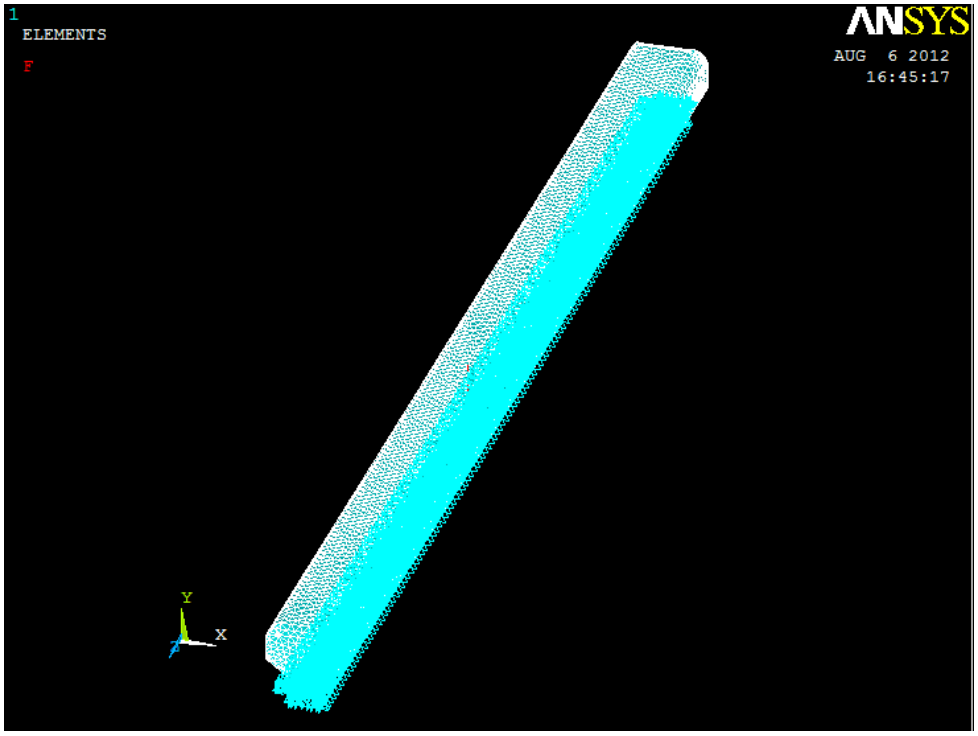

Figure 5.4: Displacement boundary conditions on the rail foot

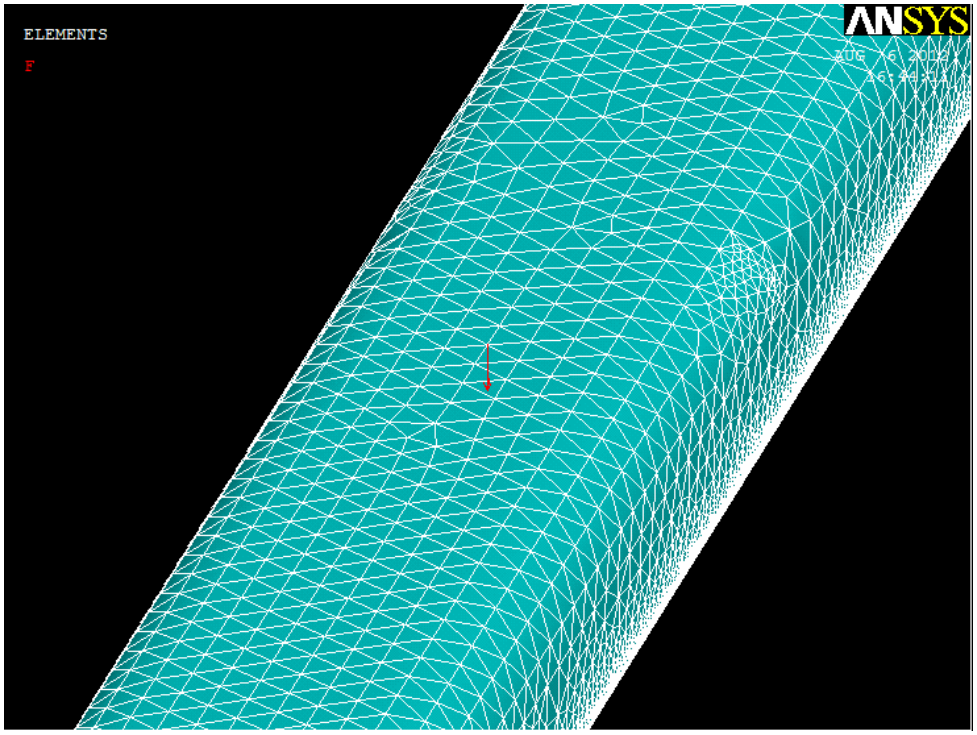

Figure 5.5: Load applied on the center of rail head

Chapter 6

6. Results and Discussion

6.1. Position of Contact Point

- ✓ When $s_2{}^{w} = 90^{\circ}$ or 270°

This result shows that at the normal condition (normal wheel/rail interaction) the wheel profile coordinates must be perpendicular to each other. However, if the value of $s_2{}^{w} \neq 90^{\circ}\ or\ 270^{\circ}$ due to plastic flow of the contacting surfaces, the wheel profile will be distorted which results the condition of multi point contact even it will be changed to conformal contact (area contact).

Therefore from this result it is possible to conclude that the wheel/rail contact at the normal condition is pure non-conformal contact which results the point or line contact depending on the arrangement and shape of wheel and rail. However, in this paper the arrangement of the wheel and rail is crossing arrangement and the shapes of the two bodies are different. Due to these, the contact condition between them is point contact.

- ✓ When $s_2{}^{r} = 0$

It implies that, the contact point on the rail surface is on the center of rail head (on the rail space curve). It is the design value expected for safe and prolonged operations of railway vehicle. However, it can be affected due to improper installation of the track.

- ✓ When $s_1{}^{w} = \frac{p_1(a_2b_3+a_3b_2)-(p_1b_2a_3+a_3a_2p_2)}{a_2(a_2b_3-a_3b_2)}$

$s_1{}^{w}$ is different from zero which shows that the positions of contact points on the wheel surface along the wheel lateral direction depends on the orientation of the three Euler angles. Therefore the position of wheel lateral contact points depends on:

- ✓ The supper elevation
- ✓ The wheel set arrangement
- ✓ The wheel set orientation
- ✓ The rail track curvature (the yaw angle)

6.2. Stress Level Results on the Contact Point with ANSYS (13)

6.2.1. Principal Stress (σ_1) and (σ_2)

Based on the Hertz contact theory for point contact, principal stress (1) and (2) are assumed to be equal. Based on his theory of contact, the point contact is occurred on sphere to sphere contact model. Therefore for sphere-sphere contact model there are two planes of symmetry in loading. Two planes of symmetry in loading and geometry dictates that principal stress (1) and (2) are equal. However, in ANSYS simulation result, node-node contact, the values of the principal stresses (1) and (2) are different at different positions of nodes within the contact point as seen in the following figures. This is due to the enlargement of the contact point to the extent of visible contact patch shape which has many nodes per contact. The directions of the planes of the two principal stresses are basically different due to that the position, magnitude, and direction of those stresses will be different throughout the shape of the contact patch.

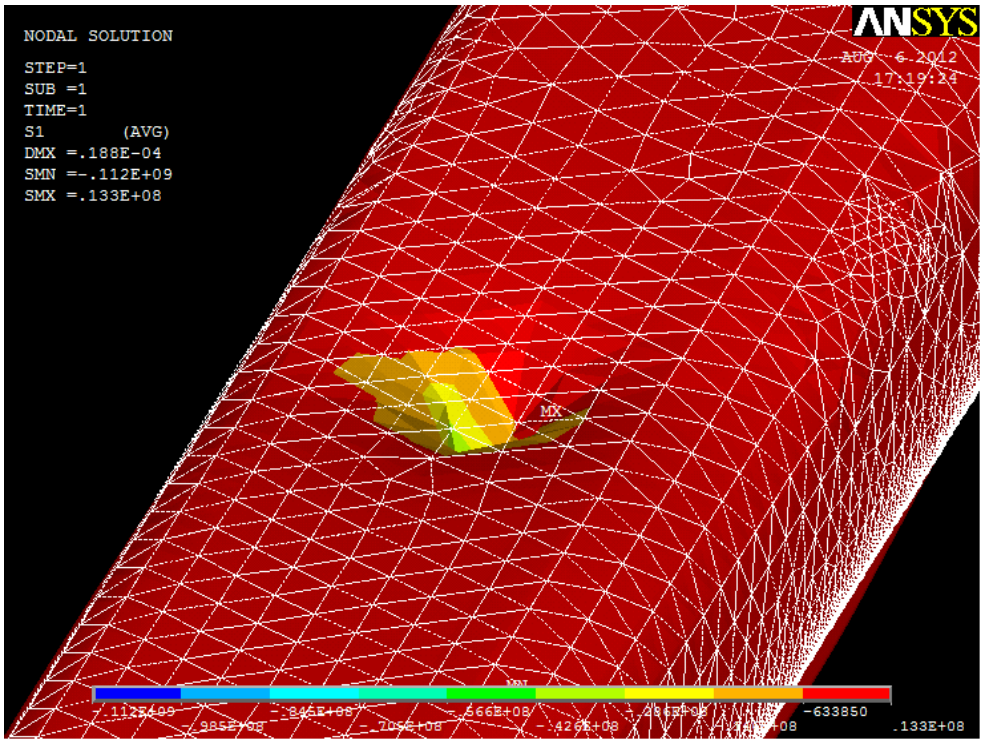

Figure 6.1: Principal stress (σ_1) distribution on the point contact patch

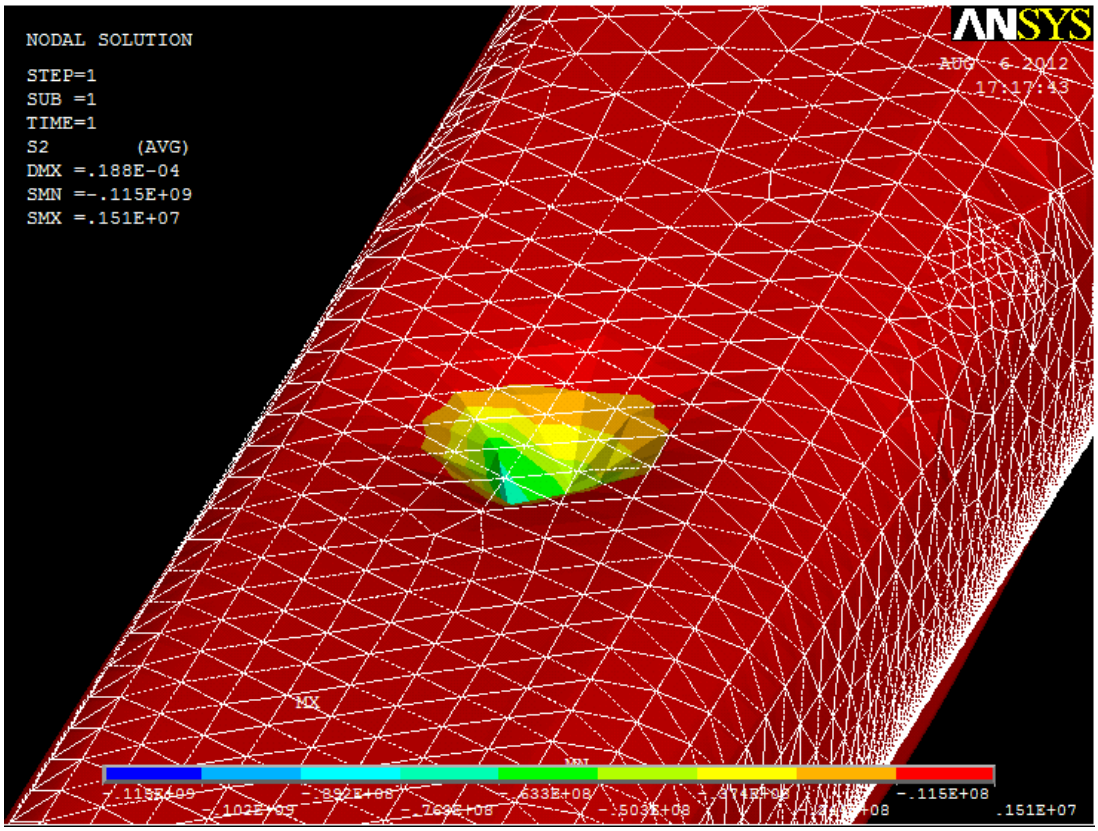

Figure 6.2: Principal stress (σ_2) distribution on the point contact patch

6.2.2. Principal Stress (σ_3)

The principal stress (σ_3) is the stress result along the line of load application. Therefore it is the maximum stress of all the stresses on the area of contact patch. As it is simple to see the principal stress (3) simulation result indicates the stress level of each sub surfaces. The outer layer of the rail head surface experiences the higher stress level and the stress level decreases down to the sub surfaces.

Generally the principal stress has a low stress distribution values when it goes far away from the center of the contact point (the stress value decreases as the contact radius increases). However it has a higher value on the center of the contact patch (it has maximum stress values when the contact point radius approaches zero).

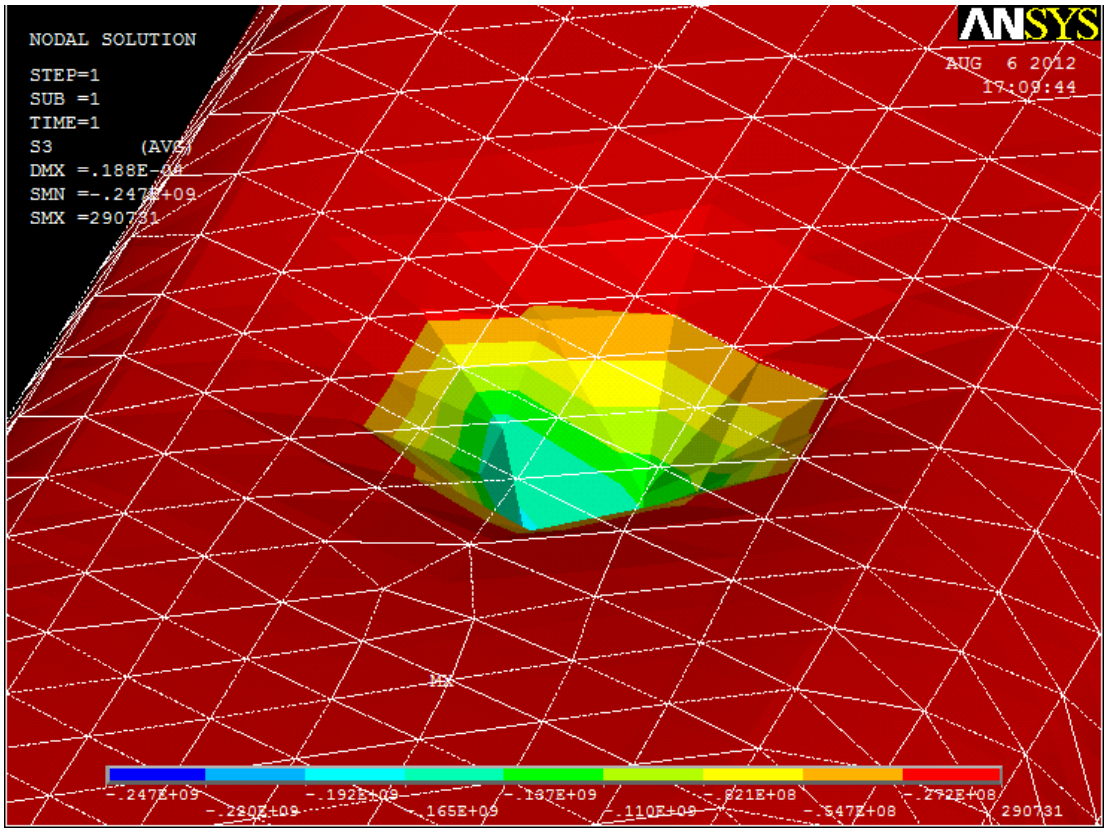

Figure 6.3: Principal stress (σ_3) distribution on the point contact patch

6.3. Stress Distributions on the Rail Head with MATLAB (7.6)

6.3.1. Maximum Principal Stress ($\sigma_3 = \sigma_z$) Distribution

According to [13] the normal load on the wheel-rail point contact is in the range between (600-800 MPa). By considering the Hertz point contact model (sphere-sphere), in this paper the maximum principal stress distribution with the maximum contact pressure of $794.9\ MPa$ which is in the range of normal load between (600-800 MPa) is normally fit to Hertz stress distribution results. Based on this result the maximum contact stress occurs on the centers of the rail head which is on the space curve of the rail head. The maximum stress distribution decreases when it goes far away from the center of the contact patch implies that far away from the center of the rail head.

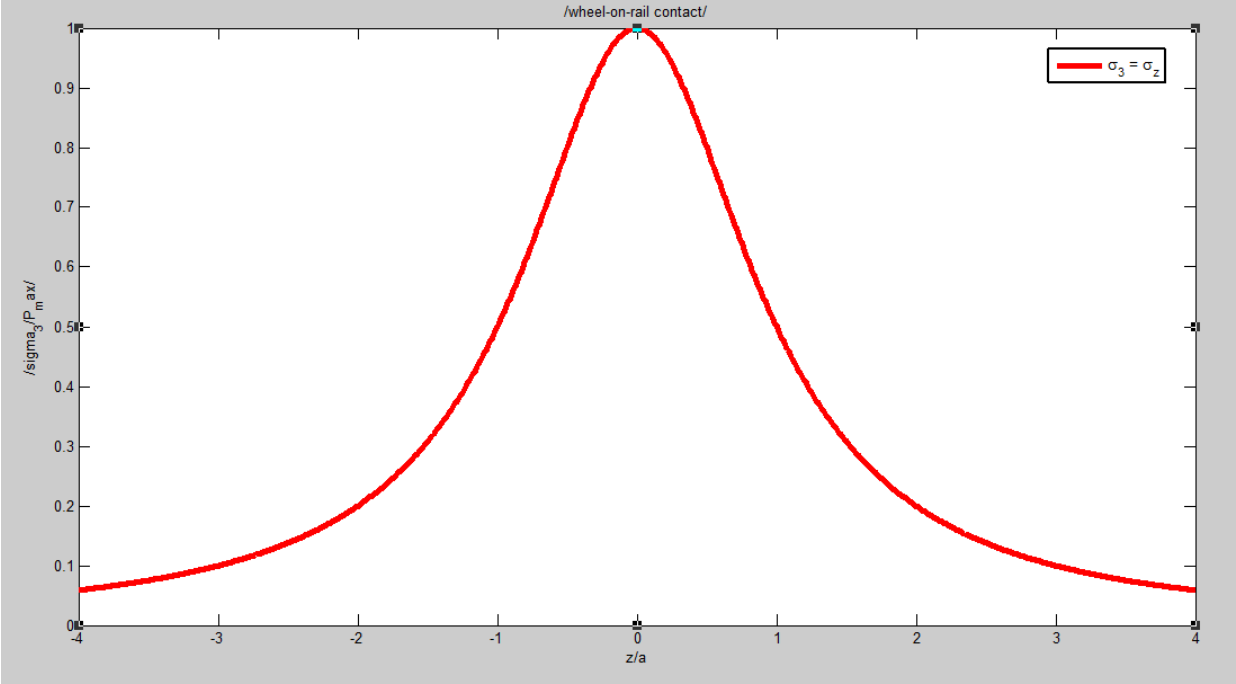

Figure 6.4: Maximum principal stress distributions along the axis of major contact radius

6.3.2. Principal and Shear Stresses Distribution

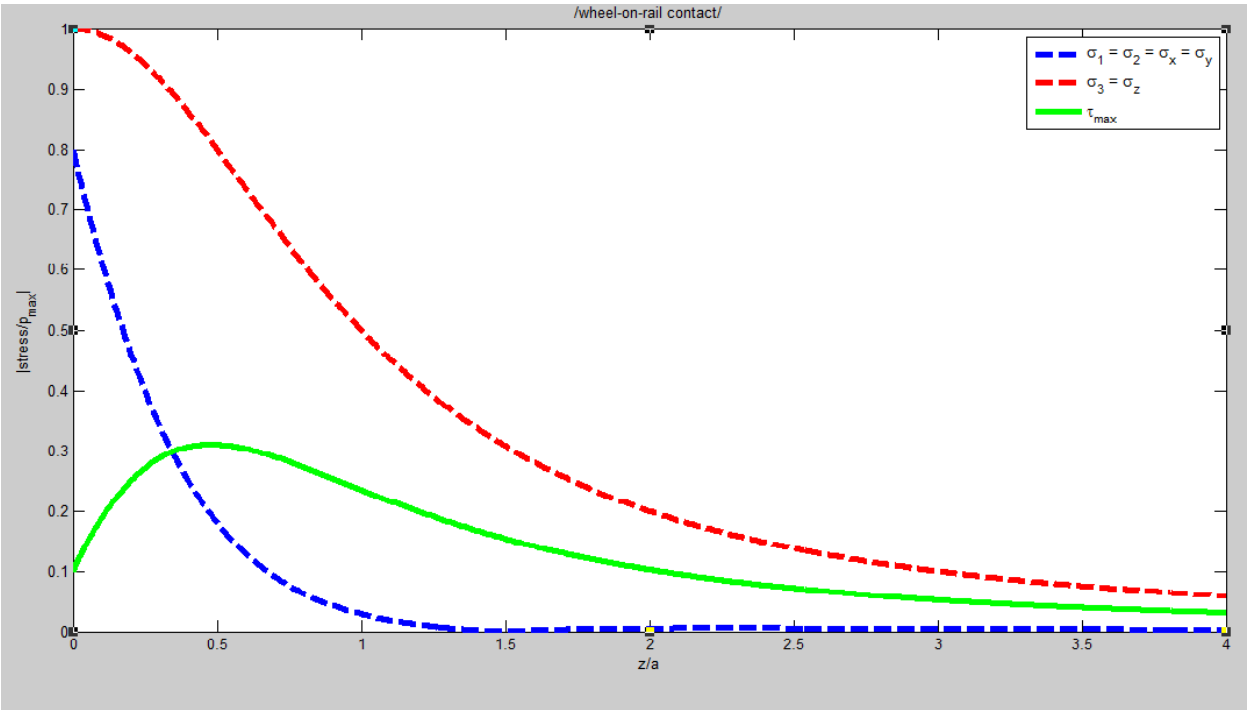

Figure 6.5: Principal and shear stresses distributions along the half length of major contact radius

These figures (Fig 6.6 and Fig 6.5) show the distribution of different stresses on the wheel-rail contact point comparing with each other. It indicates that on the center of the contact point the principal stress is maximum and the shear stress is minimum, approximately zero. But at approximately around absolute value of z=0.5a the shear stress is maximum and can be evaluated by using the values of principal stresses (1) and (2). As explained in figure 5.1 the maximum shear stress occurs on a plane oriented at an angle 45 degrees.

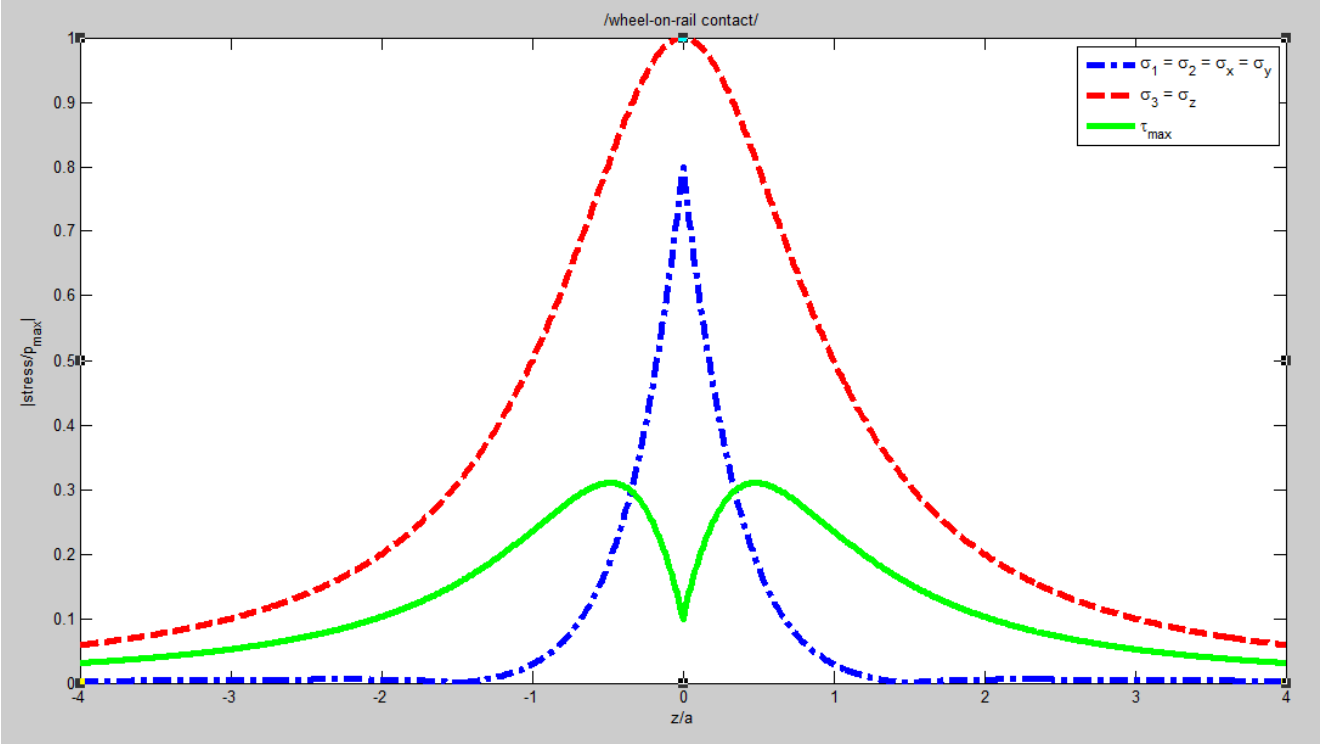

Figure 6.6: Principal and shear stresses distributions along the axis of major contact radius

6.3.3. Stress Distribution along the Depth of the Contact Point

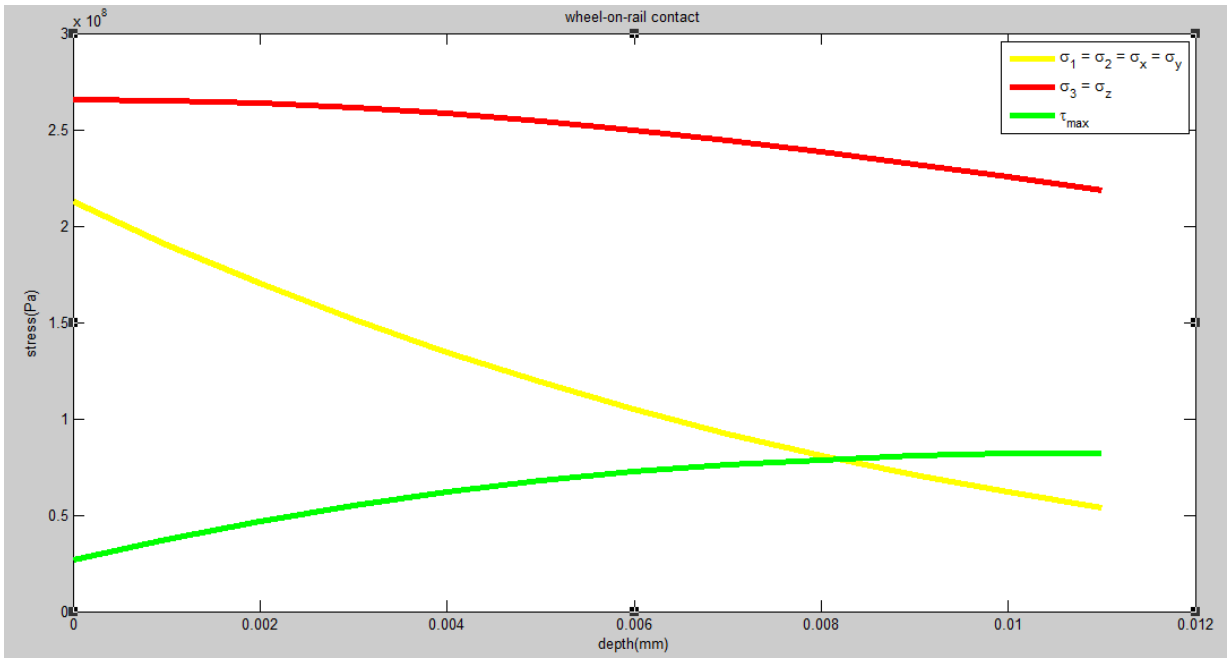

Figure 6.7: Stress Vs contact point depth

6.3.4. Effects of Applied Load on Maximum Pressure Distribution

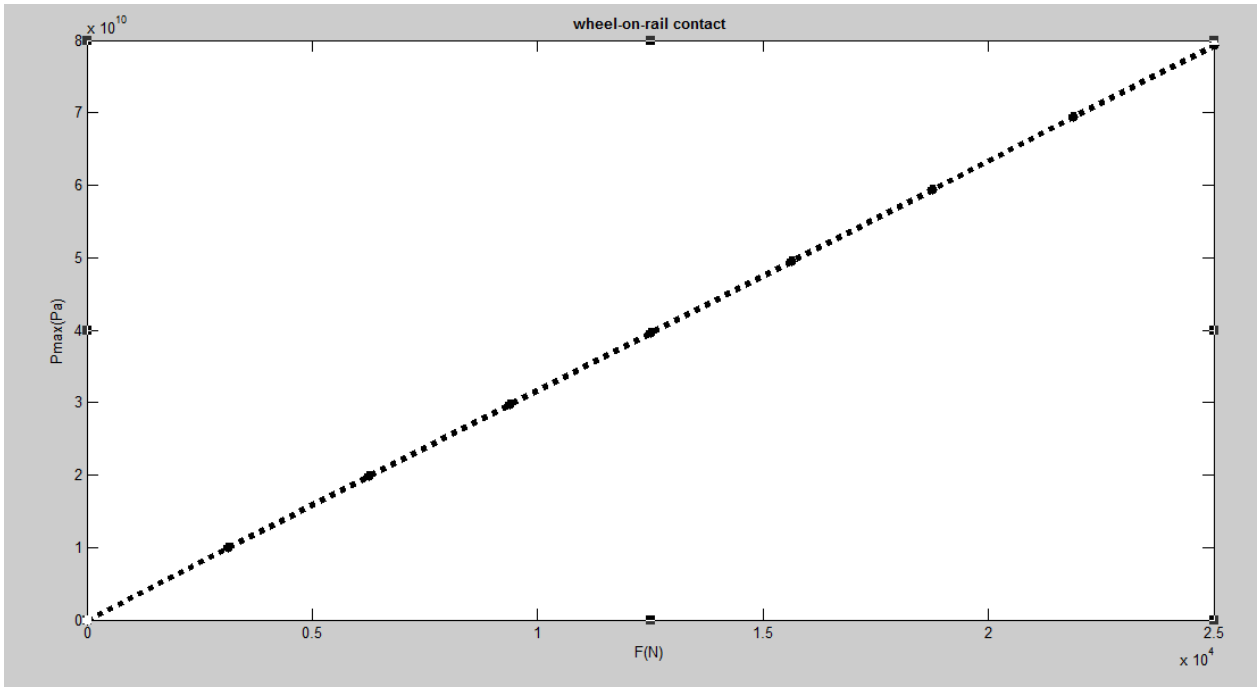

Figure 6.8: Applied load Vs maximum pressure

6.3.5. Effects of Applied Load on Contact Radius

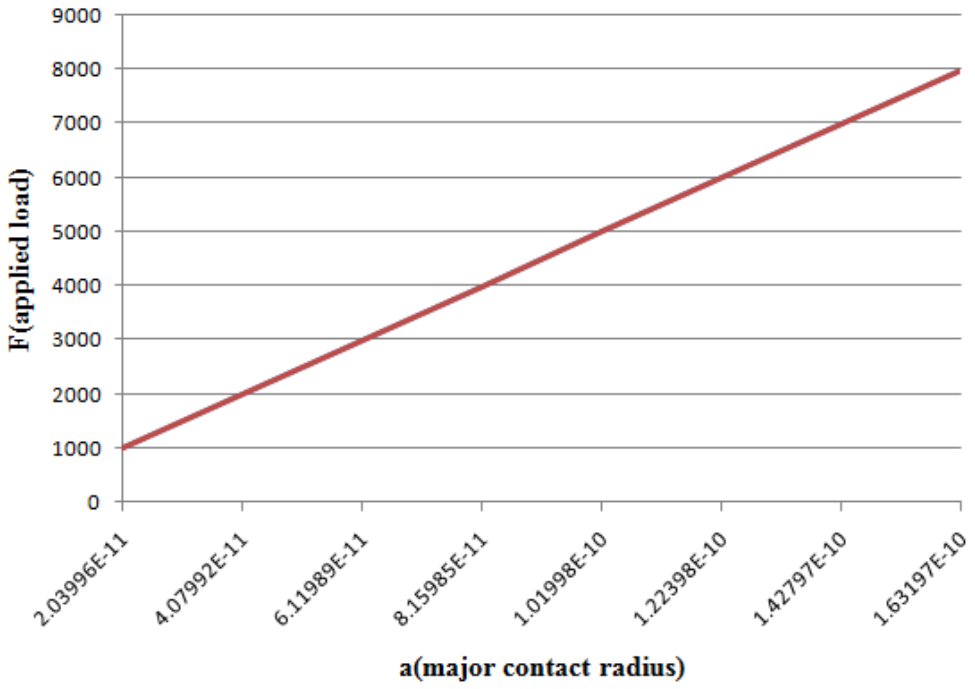

Figure 6.9: Major contact radius Vs applied load

6.3.6. Effects of Contact Radius on Maximum Pressure Distribution

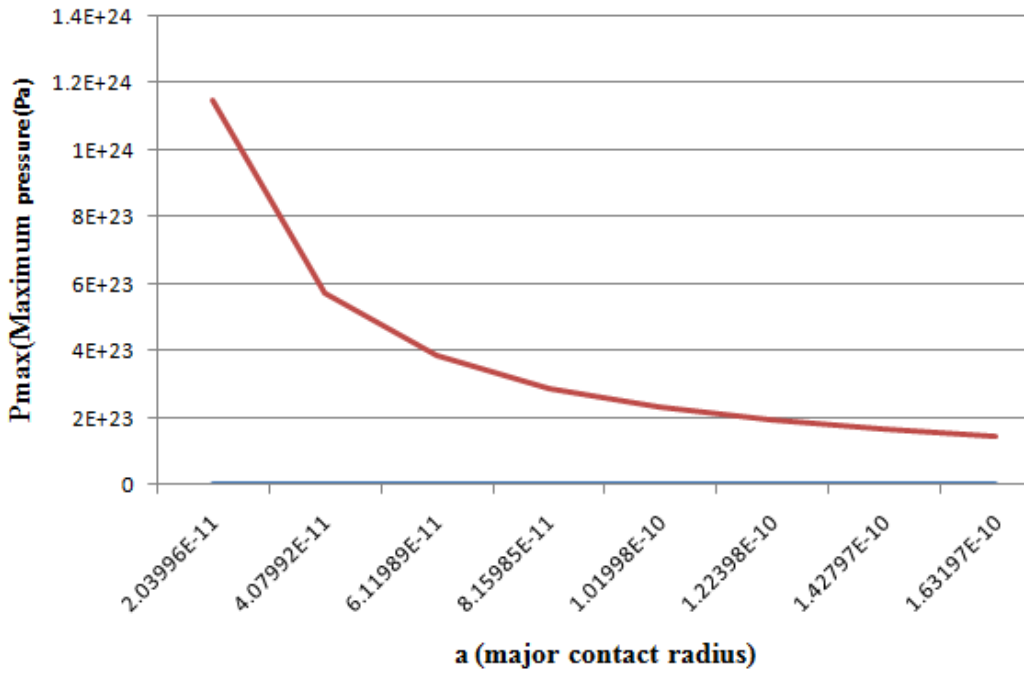

Figure 6.10: Major contact radius Vs maximum pressure

6.4. Summary

The railway wheel/rail interactions have different problems like stability and damage problems on the interface of the two components. Therefore, to show the methods of solutions for such kind of problems it is mandatory as rule and procedure to identify the type of interaction, the position of interaction, the causes of those damages etc. of the two bodies. In this paper the first priority is given to the analysis of wheel/rail contact geometry and searching of positions of contact points on the rail head surface. The result of searching of positions of contact points by developing mathematical models show that the rail space curve (rail longitudinal centerline) is the place of contact between the wheel/rail interactions. On this point from the analytical results obtained, the contact point determining parameter s_2^r is zero which indicates that if there is a proper wheel arrangements and installation of rail track, the interaction between them is a point contact and it is on the center of rail head. But the position of contact points on the wheel lateral surface depends on the positions of wheel and the orientation of rail tracks.

From the simulation results of ANSYS (13) and MATLAB (7.6) the main causes of problems (damage and instability) are basically unbalanced stresses (shear and normal). This is due to improper engagement of wheel and rail which depends on the design and installation defaults.

In this paper the stresses identified are principal and shear stresses. Based on the contact theory of Hertz the region where those stresses distribute and had effects on the material is basically elliptical. This is due to the general wheel/rail geometry and arrangements. On the center of the contact region that is when the radius of the contact ellipse approaches to zero the main causes of problems is the principal stress especially the maximum principal stress. The maximum principal stress is the stress along the load application. However it doesn't mean that the remaining principals stresses have no effect, they will have the combined effect on the rail head surface. As the radius of the contact ellipse increase along the width and longitudinal direction of the rail head the value of the principal stresses decreases. Inversely, the value of maximum shear stress is zero on center of the contact region and maximum on the plane which is oriented at around 45 degree from the principal stress plane. The axle load applied on the rail head is 25000 N as stated in table 5.1. According to Pau [13] the normal pressure which can be carried by the rail head during wheel/rail interaction is in the range (600-800 MPa). From the analytical result obtained, the maximum pressure due to 25000 N axle load is 794.9 MPa which is included in the range specified.

Chapter 7

7. Conclusion and Future Works

7.1. Conclusions

From the analysis of wheel/rail contact geometry with specified conditions the type of interaction (contact) is computed analytically and identified as point contact that is on the centerline of the rail head at the point where the lateral rail parameter ($s_2{}^r$) is zero. However, the respective contact point on the wheel surface depends on the wheel arrangements and rail track orientations. It varies across the running surface of the wheel depending on the relative positions of the wheel set.

The shape of contacting patch is calculated as elliptical, this is based on the assumptions taken at the beginning of the paper work. The general assumptions are based on the Hertz contact theory. Therefore based on those assumptions and mathematical models developed, the shape of this very small contact patch is elliptical. Its size depends on the load applied, very small like finger nail when the load applied is on normal range, and its size will increase if the load applied is out of range.

The maximum pressure distribution on this elliptical contact patch is assumed to be uniform pointing its extreme value on the center of the contact patch where the radii of the contact patch approaches zero and finite on the circumference of the ellipse. The value of average maximum contact pressure on the whole area of ellipse (contact patch) is $794.9\ MPa$. This is due to the axle load (25000 N) transmitted from single railway wheel.

The stresses identified on the contact point causing future failures (wear, fatigue and instability) are shear and principal stresses. From the simulation results conducted in the previous chapter the direction and the point where their extreme values happened are different. On the center of the contact patch where the radii of ellipse approaches zero the first failure causes is identified as maximum principal stress ($\sigma_3 = \sigma_z$). In addition to (σ_3) principal stress (σ_1 and σ_2) have the combined effect on this point. However along the lateral and longitudinal directions which are far away from the center of the contact patch the whole values of principal stresses are minimum. Inversely, the value of maximum shear stress is minimum on the center of the contact patch and maximum on a plane oriented 45 degree from the plane of principal stresses.

7.2. Future Works

During the analysis of wheel/rail contact, there are a lot of problems to be solved. However, due to the broad applications of wheel/rail contact mechanics, in this paper the analysis is limited to the geometry of wheel/rail contact just to locate the position of contact and to show the effect of applied axle load on the rail head surface.

During the work of this paper and review of literatures there are a lot of related problems expected to be solved parallel or after the accomplishment of this paper. However, expecting that, identifying the place of failure and failure causes play a great role on the future works of minimizing wheel/rail contact problems, this paper gives priority for the analysis of wheel/rail contact and applied load conditions on the rail head surface.

Based on the current and future railway demands and expected shortage of raw materials in the world and in our country Ethiopia, the broad study of contact mechanics invites the future works of researchers, especially on wheel/rail contact mechanics. Although there are so many problems on the wheel/rail contact mechanics, it will be better to group them into two major categories.

1. Stability problems
    - ✓ Optimizing rail web deflection
    - ✓ Analysis of Wheel and rail Surface irregularities
    - ✓ Stability analysis of railway bogies
    - ✓ Wheel/rail shape optimization for a specific application
    - ✓ Design of wheel derailment preventive mechanism etc.
2. Damage problems
    - ✓ Identifying the type of stress induced on the wheel/rail contact interface
    - ✓ Developing materials with cyclic load resistance
    - ✓ Determining optimum rail head surface layer etc.

References

[1].Golubenko, A., S. Sapronova, and V.Tkachenko (2007). Kinematics of Point-to-Point Contact of Wheels With a Rails. Transport Problems. East Ukrainian Volodymyr Dal National University.

[2]. Escalona, J. and R. Chamorro (2008). Efficient On-Line Calculation of the Wheel-Rail Contact Forces in Multibody Dynamics. Symposium of Advances in Contact Mechanics. Delft, The Netherlands.

[3].Kumaran, G., D. Menon and K.K. Nair (2003). Dynamic Studies of Rail Track Sleepers in a Track Structure System. Journal of Sound and Vibration. 268: 485-501.

[4].Shevtsov, I.Y., V.L. Markine and C. Esveld (2003). Optimal Design of Wheel Profile for Railway Vehicle. Conference on Contact Mechanics and Wear of Rail/Wheel Systems. Gothenburg, Sweden June 10–13, 2003.

[5]. Evans, J. R., T.K.Y. Lee, and C.C. Hon (2008). Optimising the Wheel/Rail Interface on a Modern Urban Rail System.Vehicle System Dynamics. 46:51, 119-127.

[6].Pombo, J., J. Ambrósio and M. Silva (2007). A new Wheel–Rail Contact Model for Ralway Dynamics. International Journal of Vehicle Mechanics and Mobility. 45:2, 165-189.

[7]. Kaewunruen, S. and A.M. Remennikov (2008). Dynamic Properties of Railway Track and its Components : A State-of-The-Art review. Faculity of Engineering Papers. University of Wollongong.

[8]. Karwacki, J. and S. Duda (2009). Methodology for the Dynamic Analysis of the Single Wheelset Rrunning on Turnout. Modeling and Optimization of Physical Systems. 8: 23-28.

[9]. Kataoka, H. (2008). Design Concept and Material Demand Characteristics of Rail. Welding International . 22:6, 411-415.

[10]. Knothe, K. (2008). History of Wheel/Rail Contact Mechanics: From Redtenbacher to Kalker, Vehicle System Dynamics. International Journal of Vehicle Mechanics and Mobility . 46:1-2, 9-26.

[11]. Povilaitiene, I. and A. Laurinavičius (2004). Reduction of external rail wearing on road curves. Journal of Civil Engineering and Management. 10:2, 123-130.

[12]. Eickhoff, B.M. (1993). Wheel/Rail Interaction. British Rail Research . Track Technology Course.

[13].Pau, M., F. Aymerich and F. Ginesu (2002). Distribution of Contact Pressure in Wheel–Rail Contact Area. Wear. 253 : 265-274.

[14]. Polach, O. (2009). Characterstic Parameters of Nonlinear Wheel/Rail Contact Geometry. Proceeding of the 1st IAVSD Symposium, Stockholm. 17-21 Augest, 2009. Paper No. 95.

[15]. Matsumura, R., H. Sugiyama and Y. Suda (2011). Analysis of Vehicle/Turnout Interactions of Railroad Vehicles Using Multiple Contact Tables. Journal of System Dsign and Daynamics. 5: 3.

[16]. Frich, A. and Dr. Wolfgang, S. (2008). Target Profiles for Grinding A Never Ending Story. ARM Conference. Swedish Rail Administration.

[17].Yan, W. and D. Fischer (2000). Applicability of the Hertz contact theory to rail-wheel Contact problems. Archive of Applied Mechanics. 70: 255-268.

[18]. _____., (2012). History of Rail Transport. Wikipedia, The Free Encyclopedia. http://en.wikipedia.org/wiki/History_of_rail_transport. Accessed Date, 23-10-2012.

[19]. _____., (2012). Rail Transport in Ethiopia. Wikipedia, The Free Encyclopedia. http://en.wikipedia.org/wiki/Rail_transport_in_Ethiopia. Accessed Date, 23-10-2012.

ADDIS ABABA UNIVERSITY

SCHOOL OF GRADUATE STUDIES

INSTITUTE OF TECHNOLOGY

DEPARTMENT OF MECHANICAL ENGINEERING

DECLARATION

I, the undersigned, declare that this thesis is my original work and has not been presented for any degree in any university and all the sources of materials used for the thesis have been duly acknowledged.

Addisu Negash _____ _____

Name Signature Date

October, 2012